Chapter one

Introduction

The major goal of radiation therapy is the delivery of a prescribed radiation dose as accurate lays possible to a tumor region while minimizing the dose distribution to the neighboring normal tissues. There are several geometric factors which tend to compromise this goal such as patient movement, improper placement of shielding blocks, shifting of skin marks relative to internal anatomy and incorrect beam alignment. At present, the only method commonly available for measuring and documenting the extent of geometric treatment accuracy is the radiotherapy portal film. These films are used by most radiotherapy institutions to evaluate the degree to which the actual delivered radiation therapy matches the planned treatment.

1.1 Problem of the study

In radiotherapy the physician used different filed sizes to treat cancer tissues. In cobalt 60 the field size associated with penumbra, which added radiation to the patient outside the treatment field, as well the radiation field itself located on the skin surface of the patient using a light beam to simulate the radiation. The radiation field must have a uniform radiation all over the radiation field. Therefore assessment of all these parameter is important for proper treatment process.

1.2 Research questions:

● is it possible to have best assessment of radiotherapy treatment field?

● Dose this method give the exact determination of radiation field size and penumbra size?

● Dose this method give the correct value of uniformity?

1.3 Objectives:

The general objective of this study is to assess the radiation field of the Co-60 and linear accelerator on portal film using image processing to have an objective and quantitative measures.

Specific objectives

- To identify the Region Of Interest (ROI), radiation field and penumbra size
- To check the accuracy of the treatment field
- To measure the penumbra size
- To calculate the uniformity of the treatment field

1.4 The methodology

IDL, short for Interactive Data Language, is a programming language used for data analysis. It is popular in particular areas of science, such as astronomy and medical imaging. IDL shares a common syntax with PV-Wave and originated from the same codebase. IDL is vectorized, numerical, and interactive, and is commonly used for interactive processing of large amounts of data (including image processing). The syntax includes many constructs from FORTRAN and some from C.

IDL originated from early VAX/VMS/Fortran, and its syntax still shows its heritage:

```
x = findgen (100)/10
y = sin(x)/x
```

```
Plot, x, y
```

The findgen function in the above example returns a one-dimensional array of floating point numbers, with values equal to a series of integers starting at 0.

Note that the operation in the second line applies in a vectorized manner to the whole 100-element array created in the first line, analogous to the way general-purpose array programming languages (such as APL, J or K) would do it. This example contains a divide by zero; IDL will report an arithmetic overflow, and store a NaN value in the corresponding element of the y array (the first one), but the other array elements will be finite. The NaN is excluded from the visualization generated by the plot command.

As with most other array programming languages, IDL is very fast at doing vector operations (sometimes as fast as a well-coded custom loop in FORTRAN or C) but quite slow if elements need processing individually. Hence part of the art of using IDL (or any other array programming language, for that matter) for numerically heavy computations is to make use of the built-in vector operations.

IDL is not simply a package of task-oriented routines in the style of astronomical software systems such as IRAF or CIAO. Instead, it is genuinely a computer ***language***, readily understandable by any computer-literate user. It offers all the power, versatility, and programmability of high level languages like FORTRAN and C. But it incorporates three special capabilities that are essential for modern data analysis:

- ***interactivity***,
- ***graphics display***, and

- ***Array-oriented operation***. (IDL is array-oriented in the sense that arrays can be referenced without the use of subscripts or do-loops and that code is automatically vectorized for fast array computations.)

Users who are conversant with FORTRAN, C, C++, or other high level languages will have little trouble understanding IDL. Its syntax and operation are clear, sensible, and convenient (most similar to FORTRAN's). Because it is interactive, learning IDL through on-line trial-and-error is rapid.

IDL provides the scientist better understanding of and control over computations and data analysis by virtue of a large number of special feature.

1.5 Significance of the study

For accurate treatment process, the radio therapy beam must be assessed using suitable method to ensure that specific dose selectively delivered to the intended organ, and to achieve the goal of radiotherapy that the maximum dose is on the tumor where the minimum dose on the surrounding tissue.

Chapter two

Literature review

2.1.1 External beam radiotherapy (EBRT) or teletherapy:

Is the most common form of radiotherapy ,The patient sits or lies on a couch and an external source of radiation is pointed at a particular part of the body. In contrast to internal radiotherapy (brachytherapy), in which the radiation source is inside the body, external beam radiotherapy directs the radiation at the tumor from outside the body. Kilovoltage ("superficial") X-rays are used for treating skin cancer and superficial structures. Megavoltage ("deep") X-rays are used to treat deep-seated tumors (e.g. bladder, bowel, prostate, lung, or brain).

In the medical field, useful X-rays are produced when electrons are accelerated to a high energy. Some examples of X-ray energies used in medicine are:

- Diagnostic X-rays - 20 to 150 kV
- Superficial X-rays - 50 to 200 kV
- Orthovoltage X-rays - 200 to 500 kV
- Supervoltage X-rays - 500 to 1000 kV

Megavoltage X-rays - 1 to 25 MV

Megavoltage X-rays are by far most common in radiotherapy for treatment of a wide range of cancers. Superficial and orthovoltage X-rays have application for the treatment of cancers at or close to the skin surface.

Medically useful photon beams can also be derived from a radioactive source such as iridium-192, caesium-137 or radium-226 (which is no longer used clinically), or cobalt-60. Such photon beams, derived from radioactive decay, are more or less monochromatic and are properly termed gamma rays. The usual energy range is between 300 Kev to 1.5 MeV, and is specific to the isotope.

Therapeutic radiation is mainly generated in the radiotherapy department using the following equipment:

-Orthovoltage units. These are also known as "deep" and "superficial" machines depending on their energy range. Orthovoltage units have essentially the same design as diagnostic X-ray machines. These machines are generally limited to less than 600 kV.

-Linear accelerators ("linacs") which produce megavoltage X-rays. The first use of a linac for medical radiotherapy was in 1953 (see also radiotherapy). Commercially available medical linacs produce X-rays and electrons with an energy range from 4 MeV up to around 25 MeV. The X-rays themselves are produced by the rapid deceleration of electrons in a target material, typically a tungsten alloy, which produces an X-ray spectrum via bremsstrahlung radiation. The shape and intensity of the beam produced by a linac may be modified or collimated by a variety of means. Thus, conventional, conformal, intensity-modulated, tomographic, and stereotactic radiotherapy are all produced by specially-modified linear accelerators.

-Cobalt units which produce stable, dichromatic beams of 1.17 and 1.33 MeV, resulting in an average beam energy of 1.25 MeV. The role of the cobalt unit has partly been replaced by the linear accelerator, which can generate higher energy radiation. Cobalt treatment still has a useful role to play in certain applications (for example the Gamma Knife) and is still in widespread use worldwide, since the machinery is relatively reliable and simple to maintain compared to the modern linear accelerator.

2.1.2 Digital image processing:

Is the use of computer algorithms to perform image processing on digital images. As a subcategory or field of digital signal processing, digital image processing has many advantages over analog image processing. It allows a much wider range of algorithms to be applied to the input data and can avoid problems such as the build-up of noise and signal distortion during processing. Since images are defined over two dimensions (perhaps more) digital image processing may be modeled in the form of multidimensional systems. Many of the techniques of digital image processing, or digital picture processing as it often was called, were developed in the 1960s at the Jet Propulsion Laboratory, Massachusetts Institute of Technology, Bell Laboratories, University of Maryland, and a few other research facilities, with application to satellite imagery, wire-photo standards conversion, imaging, videophone, character recognition, and photograph enhancement. The cost of processing was fairly high, however, with the computing equipment of that era. That changed in the 1970s, when digital image processing proliferated as cheaper computers and dedicated hardware became available. Images then could be processed in real time, for some dedicated problems such as television standards conversion. As general-purpose computers

became faster, they started to take over the role of dedicated hardware for all but the most specialized and computer-intensive operations.

With the fast computers and signal processors available in the 2000s, digital image processing has become the most common form of image processing and generally, is used because it is not only the most versatile method, but also the cheapest.

Digital image processing technology for medical applications was inducted into the Space Foundation Space Technology Hall of Fame in 1994.

In 2002 Raanan Fattal introduced Gradient domain image processing, a new way to process images in which the differences between pixels are manipulated rather than the pixel values themselves.

2.1.3 Field Size:

Is the measure of an area irradiated by a given beam, there are two most useful conventions.

The first is the geometric field size; The geometric projection on a plane perpendicular to the central ray of the distal end of the collimator as seen from the center of the front surface of the source. The second is the physical field size, defined as the area included within the 50 percent maximum dose isodose curve at the depth of maximum dose.

2.1.4 penumbra size:

The penumbra for electron beams is defined either in terms of the distance between two isodose values on a beam profile at the depth of maximum dose (or at the standard measurement depth), or indirectly in terms of distances between specified isodoses and the geometric field edge under stated conditions as above. If the former, then generally the 20%–80% width is expected to be 10 mm to12

mm for electron beams below 10 MeV, and 8 mm to10 mm for electron beams between 10 MeV and 20 MeV. These values apply for applicators with the final collimation stage at 5 cm or less from the skin, but for greater separation between the applicator and the skin the penumbra will increase.

2.2 previous studies :-

Yousif M et al,(2014), assessed the field size on radiotherapy machines using texture analysis, by using image processing technique and for radiotherapy machines (Co-60 and linear accelerator), each film scanned using digitizer scanner then treat using image processing program Matlab, where the congruence of the light and radiation field should be determined. The scanned image saved in a TIFF file format to preserve the quality of the image. The data analyzed include upper, lower, right, and left borders of the light and radiation field in megavoltage films. The result showed that the mean light field size was 10.0 × 10.1 cm, medical physicist score was 10.2 ± 0.11608 cm × 10.2 ± 0.099861 cm, and the field size that calculated by computerized score using Matlab program was 9.9 ± 0.36049 cm × 9.9 ± 0.1123 cm, the result also showed that the computerized score is more accurate in determining of borders and penumbra than medical physicist score.

Lin et al, (2000). By Thermopile detectors the spatial non-uniformity measured and with correction methods. The spatial non-uniformity of a newly developed electrically calibrated radiometer system is characterized. The detector is a thin-film thermopile with an integral electrical heater. The local responsivities of these detectors have a rotational symmetry and a quadratic dependence on the distance to the center of the detector. Typical measurement errors, which can be

caused by applying different beam sizes, different power distributions of the beams, and different beam positions impinging on the detector, are investigated. A significant reduction of measurement uncertainties is achieved using specific corrections. The influence of spatial non-uniformity on responsivity measurements is experimentally checked with various types of beam.

Leszczynski KW et al, (2003), Verified radiotherapy treatments: computerized analysis of the size and shape of radiation fields. An automated technique has been developed for the verification of treatment field size and shape in external beam radiation therapy. Portal images from film or digital on-line imaging system are analyzed, and basic parameters are derived to describe the field size and shape from the contour points on the field boundary. The initial set of parameters included length of the perimeter, area, aspect ratio, and orientation angle. The parameters found for the actual field in the portal image are compared against those calculated for the prescribed field and any discrepancies indicated to the operator. The accuracy of the field parameterization scheme has been tested on a number of on-line portal images with varying fields. The relative error did not exceed a few percent in perimeter and area or 2 degrees in the angle, which should be sufficiently low for the detection of major errors in field shaping.

Se An Oh et al. (2012), Studied penumbra for high-energy photon beams with Gafchromic™ EBT2 films using the Pencil Beam Convolution algorithms and self-developing Gafchromic™ EBT2 film. For dose calculations and EBT2 measurements, they used an acryl phantom with dimensions 20 × 20 × 20 cm3. The 200 cGy dose was delivered to the central depth (10 cm) of the acryl

phantom. The result of this study was that increased energy, field size and depth are rise to an increased penumbra (20% ~ 80%) width. For a 6 MV photon energy, the penumbra widths (20%–80%) at 1.5 cm, 5 cm, and 10 cm depths were 4.2 mm, 4.4 mm, and 5.7 mm for the eclipse calculations and 2.9 mm, 4.1 mm, and 4.2 mm for the EBT2 film measurements for 10 × 10 cm2 field sizes, respectively. For a 10 MV photon energy, the penumbra widths were 4.5 mm, 4.7 mm, and 6.2 mm for eclipse calculations and 4.1 mm, 4.6 mm, and 4.9 mm for EBT2 film measurements, respectively. As the field size was changed to 3 cm, 5 cm, 7 cm, 10 cm, and 15 cm, the penumbra widths changed to 5.1 mm, 5.3 mm, 5.6 mm, 5.9 mm, and 6.1 mm for eclipse calculations and 2.9 mm, 3.3 mm, 3.6 mm, 4.2 mm, and 5.1 mm for EBT2 measurements, respectively, for 10 cm depths for 6 MV photon energies. In this study, compared to the 10 MV photon energy, the 6 MV photon energy was preferred in treatments such as the 3D conformal radiation therapy and the IMRT for critical organs near the target volume.

Tsang Cheung et al, (2006). Measured the high energy x-ray beam penumbra with Gafchromic™ EBT radiochromic film. Gafchromic™ EBT ISP Corp, Wayne, NJ radiochromic film is used to study penumbral doses in high energy x-ray beams. EBT film is constructed using multilayers, consisting of an active polymer coated by polyester, which allows the film to be easily handled and minimizes effects from ultraviolet exposure.14 The effective atomic number of EBT film is Zeff=6.98 and when compared to water, Zeff=7.3, provides a comparatively good match.15 Its energy dependence was found to be less than 10% over the energy range of 50 kVp to 6 MV.16 The films were used to measure penumbral regions of 6 MV x-ray beams produced by a Varian 2100EX linear accelerator. For dose delivery, the films were positioned in a solid water17 phantom with dimensions of 30 cm30

cm30 cm. The phantom was placed on the linear accelerator couch at 100 cm SSD and films were given a 2 Gy dose at the central axis using various depths for penumbral analysis. Various field sizes were tested ranging from 5 cm5 cm up to 30 cm30 cm. Measured penumbral doses were compared to the central axis dose measurements and the penumbral results quoted as 80%/20%.The Gafchromic™ EBT films were analyzed using a personal computer desktop scanner and Image J software. The scanner used was a Hewlett Packard ScanJet with a scanning resolution of 2400 pixels per inch. Analysis was performed using a 2020 pixel region of interest and provided a measurement resolution of 0.2 mm. The 16 bit images were a combination of the red, green, and blue components, with the combined image studied for analysis. Doses were calculated using a dose calibration curve produced for each field size. Less than 2% variation was seen in the dose response curves over the field sizes measured. The profile measurements of penumbra were made in the same direction as the charge coupled device CCD scanning direction. No corrections were made for transversal sensitivity of the CCD. Results were also compared to Kodak X-omat V and Kodak EDR2 radiographic film. Extrapolated, zero volume ionization chamber measurements18 were also made and compared. Radiographic film is used as a direct comparison for film dosimetry and results have been analyzed using the same densitometry system as Gafchromic™ EBT film. The extrapolated zero volume chamber results have been calculated using a technique outlined by Laub and Wong18 where a series of penumbra measurements are performed with various chambers of different spatial resolutions and an extrapolation is performed to predict the measured penumbra with a zero volume detector. Ionization chambers used in the technique were a Markus parallel plate chamber,

NE 0.6 cm3 cylindrical thimble chamber, IC13 and IC10 Wellhofer small volume ionization chambers. This technique can produce the gold standard for penumbra measurements, however, it is a very time consuming and demanding process. the percentage profile measurements at a 10 cm10 cm x-ray beam at 0.12 mm physical depth, 1.5, 5, and 10 cm depth relative to dose at the Dmax central axis as measured by Gafchromic™ EBT film. Results were normalized to 100% at central axis Dmax. The measured surface dose 0.12 mm physical depth of the EBT is approximately 22% at the central axis and slowly reduced in the peripheral regions as seen in with an increased contribution compared to dose at depth outside the treatment field. This is specifically due to the electron contamination component of the beam. Central axis %DD measurements were found to be 100%, 85%, and 66% at 1.5, 5, and 10 cm, respectively when normalized to 100% at the Dmax position. This is compared to 100%, 86.1%, and 66.1% when measured with a Farmer ionization chamber, again showing a relatively good match to chamber measurements in this region. The measured penumbra revealed a spreading which is a combination of beam divergence and increased scatter contributions at depth. Similar results were seen at other field sizes ranging from 5 to 30 cm squares. Figure 2ashows the normalized 80%/20% penumbra for the 6 MV 10 cm10 cm x-ray beam. To perform the normalization, the off axis dose is compared to the central axis dose at each specific depth and normalized to 100% at central axis. Results are shown at the surface 0.12 mm physical depth, Dmax 1.5 cm, 5, and 10 cm. The 80%/20% penumbra widths for this field size are 3.0 mm at 1.5 cm, 3.5 mm at 5 cm, and 4.4 mm at 10 cm. Similar results are shown in Fig. 2bwhich is for a 20 cm20 cm 6 MV x-ray beam. Results here are 3.1 mm at 1.5 cm, 3.7 mm at 5 cm, and 5.1 mm at 10 cm depth. Of note is the increased

peripheral dose as a ratio of the central axis for all depths, which shows a larger degree of scatter contributions in the peripheral regions from larger field sizes. Table I highlights the measured 80%/20% penumbra for various field sizes using EBT film compared to radiographic film and results from the zero volume chamber extrapolation predicted penumbra. Requires a development process. High energy x-ray beam penumbra can be accurately measured with Gafchromic™ EBT, radiochromic film

Murray A, et al, (2005), optimal uniformity index selected and acquisition counts for daily gamma camera quality control was performed, The indices were calculated for induced [localized two-dimensional (2D) Gaussian and gradient] artefacts added to three image sets (5, 10 and 15 million counts), each containing 25 extrinsic images, using Matlab. The intensity of the induced artefacts was varied between a 1 and 10% drop in pixel counts. The induced artefacts simulated photomultiplier tube [10 cm full width at half maximum (FWHM)], smaller focused artefacts (2.5 cm FWHM) and gradients artefacts.For five million count acquisitions, the Cox-Diffey, CoV and NEMA integral indices detected the 6% 2D Gaussian artefacts [10 cm full-width at half-maximum (FWHM)], whereas the NEMA differential index performed relatively poorly. NEMA differential and integral indices performed equally well at detecting smaller 2D Guassian (2.5 cm FWHM) artefacts. The 10% artefact was the minimum artefact detected by both indices for five million count acquisitions. The Cox-Diffey and CoV indices did not detect any artefacts for five million acquired counts. The CoV index performed best at detecting gradient artefacts at five million acquired counts. This provides evidence that daily quality control can be acquired with as few as five million counts while maintaining the same ability to detect both chronic and acute

nonuniformities compared with higher count acquisitions. A combination of the NEMA integral and the CoV indices gives the optimal selection of uniformity indices for detecting a range of artefact forms and intensities.

Keller et al. (2007) experimentally measured radiological penumbra associated with intermediate energy x-rays (1 MV) and small radiosurgery field sizes. Stereotactic radiosurgery is used to treat intracranial lesions with a high degree of accuracy. At the present time, x-ray energies at or above Co-60 gamma rays are used. Previous Monte Carlo simulations have demonstrated that intermediate energy x-ray photons or IEPs (defined to be photons in the energy range of 0.2-1.2 MeV), combined with small field sizes, produce a reduced radiological penumbra leading to a sharper dose gradient, improved dose homogeneity and sparing of critical anatomy adjacent to the target volume. This hypothesis is based on the fact that, for small x-ray fields, a dose outside the treatment volume is dictated mainly by the range of electrons set into motion by x-ray photons. The purpose of this work is: (1) to produce intermediate energy x rays using a detuned medical linear accelerator, (2) to characterize the energy of this beam, (3) to measure the radiological penumbra for IEPs and small fields to compare with that produced by 6 MV x rays or Co-60, and (4) to compare these experimental measurements with Monte Carlo computer simulations. The maximum photon energy of our IEP x-ray spectrum was measured to be 1.2 MeV. Gafchromic EBT films (ISP Technologies, Wayne, NJ) were irradiated and read using a novel digital microscopy imaging system with high spatial resolution. Under identical irradiation conditions the measured radiological penumbra widths (80%-20% distance), for field sizes ranging from 0.3 x 0.3 to 4.0 x 4.0 cm2, varied from 0.3-0.77 mm (1.2 MV) and from 1.1-2.1 mm (6 MV). Even more dramatic were the differences found when

comparing the 90%-10% or the 95%-5% widths, which are in fact more significant in radiotherapy. Monte Carlo simulations agreed well with the experimental findings. The reduction in radiological penumbra could be substantial for specific clinical situations such as in the treatment of an ocular melanoma abutting the macula or for the treatment of functional disorders such as trigeminal neuralgia (a nonlethal neurological pathology) where no long-term side effect should be induced by the treatment.

Kron T1 et al .(1993),The penumbra of a 6-MV x-ray beam as measured by thermoluminescent dosimetry and evaluated using an inverse square root function, Data on the dose distribution in the penumbral region of megavoltage x rays are of importance for most radiotherapy planning systems. For medical linear accelerators the distance between the points representing 20% and 80% of the central axis dose (20/80) is typically only a few millimeters. To achieve good spatial resolution a radiation detector with small physical size has to be used for penumbra measurements. The penumbra in a 6-MV therapeutic x-ray beam was investigated for field sizes of 10 x 10 cm2 and 20 x 20 cm2 at depth of maximum dose (dmax = 1.5 cm) and at 10-cm depth in a solid water phantom. In addition, the field edge of an independent jaw driven to the center of the axis of the primary collimator was investigated. LiF thermoluminescent (TL) ribbons and rods were used embedded in solid water in different geometries resulting in relative detector sizes of 1, 3.1, and 6 mm. A forming function based on an inverse square root function was used to fit the experimental penumbra measurements. For the asymmetric field an amendment to the function is proposed to give a better fit for the experimental data. From the penumbra measured with the three different detector sizes, a penumbra can be extrapolated for an infinitesimal small detector.

The extrapolated penumbral width (20/80) was found to be 2.3, 3.2, and 2.7 mm at dmax for the 10 x 10-cm2 symmetric, 10 x 10-cm2 asymmetric, and 20 x 20-cm2 field sizes, respectively. The 20/80values at 10-cm depth in the solid water phantom for the same radiation fields were 4.2, 4.3, and 4.1 mm, respectively.

Suresh Rana et al, (2013). Impact of heterogeneities on lateral penumbra in uniform scanning proton therapy, in the treatment planning of uniform scanning proton therapy, an aperture block is designed for each beam with a margin, which typically includes the lateral penumbra measured in water (homogenous) medium. However, during real proton therapy treatment, protons may pass through tissues of different densities within the patient's body before they are stopped. The main aim of this study was to investigate the dependency of lateral penumbra on low- and high-density heterogeneities placed in the plateau and spread-out Bragg peak (SOBP) regions. The measurements were performed by placing radiographic films at the isocenter (center of SOBP), and each proton beam was delivered with 150 monitor units using standard beam conditions of the institution. The preliminary, the results from this study showed that the lateral penumbra of uniform scanning proton beams was less sensitive to the inhomogeneity introduced in the protons beam path. The low-density heterogeneity in the plateau region had more impact on the lateral penumbra when compared to the low-density in the SOBP region. In contrast, the placement of high-density heterogeneity (whether in the plateau or SOBP region) produced a very minimal difference. The overall difference in lateral penumbra among different phantoms was within ±1 mm.

Hatimbhai et al, (1976), Effect of field size on the radiation penumbra and integral dose for telegamma therapy units. Because of the large source size in telegamma

therapy units, the boundaries of the radiation beam beyond the collimator are not well defined and a zone of falling dose and resulting penumbra are produced. In general, the collimator design is such that the geometrical penumbra is nearly equal in magnitude to the source diameter. However, the magnitude of the physical or radiation penumbra is influenced by the radiation transmitted through the edge of the collimator, the geometrical penumbra and the scatter from the source and the collimator. In the present study, the variation of radiation penumbra with field size has been investigated for two different makes of telegamma units. It is seen that the radiation penumbra can be as large as 4.8 cm for a 20 X 20 cm field. The effect of such large penumbra on the integral dose is discussed.

Olivia A et al. (2007), Radiation transmission, leakage and beam penumbra measured of a micro-multileaf collimator using GafChromic EBT film.Radiochromic phenomena involve the direct coloration of a material by the absorption of radiation without the use of external chemical, optical or thermal agents. Radiochromic films are nearly transparent before irradiation and consist of a micro-crystalline active thin layer based on polydiacetylene, coated on a flexible polyester film base. After irradiation, their color changes to blue due to polymerization effects. The internal structure of GafChromic EBT consists of two active layers of 17 µm thickness separated by a 6 µm layer coated on a 97 µm polyester base on each side. This design decreases the effects of environmental and ultraviolet light. (7) The atomic composition of the film material is C (42.3%), H (39.7%), O (16.2%), N (1.1%), Li (0.3%) and Cl (0.3%) with an effective atomic number of 6.98. Its sensitivity is 10 times larger than its predecessors, such as GafChromic MD- 55-2 and HS. The useful dose range is from 1 to 800 cGy, and

presents two absorption peaks at 636 and 585 nm,(12) its response is energy independent,(13) and according to the manufacturer specifications, it has a real time response. In this work, all the measurements were performed using GafChromic EBT film with serial number 36124-003I. The films were carefully handled and analyzed following the recommendations of the TG55 report (10) and those proposed by Butson and co-workers. (14) The films were placed in light-protecting envelopes, and were only removed from them during irradiation and readout, to reduce the effects of ambient light. Moreover, at all times the ambient lights were dimmed in order to avoid stray light effects. The un-irradiated films were scanned 24 h previous to irradiation and the readout was performed 48 h after irradiation, taking care of maintaining the same orientation and placement on the scanner glass tray. During the storage, irradiation, and readout the films were kept at a temperature of 21 °C and 50% humidity controlled by the cooling system of our laboratory. Readout of the EBT films was performed with a commercial flatbed scanner Scan Maker 9600XL (Microtek, USA) working in transmission mode. This scanner has a maximal optical spatial resolution of 1200×600 dpi and 36-bit color depth (12-bits per channel: red, green and blue). 36-bits color depth and 100 dpi, with all post-processing and color management options turned off. The images were stored in tagged image file format (TIFF) and analyzed using Image. (15) Only the red component of the film response was used for the analysis, due to its higher sensitivity as compared with the green and blue components. (16) In order to correct for nonuniformities caused by the light scattering of the scanner lamp (17) and intrinsic heterogeneities on the film structure, an image background correction was applied following a procedure suggested by the film manufacturer. (18) The films were digitized twice, before

and after irradiation. The non-irradiated film image (ϕo) was normalized with respect to its mean background value calculated over the entire film surface. The irradiated image (ϕi) was then corrected for non-uniformities using:

$$\varphi_c = \frac{\varphi_i}{\hat{\varphi}_o}$$

Where $\phi \hat{} o$ and ϕc correspond to the normalized and the corrected images, respectively. In order to warrant that the pre- and post- irradiation images were spatially registered, each film was marked with a fiducial and placed in the same position and orientation in the scanner glass tray. Film response was measured using the following expression (16):

$$R = \log\left(\frac{\varphi_o}{\varphi_c}\right)$$

By following the protocol for the handling and analysis of the EBT films as described in section 2, the overall one-sigma dose measurement uncertainty for a uniform field amounts to 4% or less for doses above 40 cGy. The reproducibility of the measurements reported in this work has been evaluated over a one year period and found to be within 4%. It is known that these values are specific for the type of film, digitizer and dose range used. (17, 20) In our case a document scanner was used, and a similar system used with EBT film reported overall dose uncertainties below 6% at approximately 1 Gy for a similar (single set/single scan) analysis procedure.(20) Table 4 compares the transmission and leakage radiation measurements for the m3-mMLC obtained in this work with those reported in the

literature for the same type of mMLC when using different detectors. As a reference, a couple of values for the same nominal energy and different collimator manufacturer are included in the table. It can be observed that our values are consistently lower than all the previously reported measurements using the m3-mMLC. It is important to note that the values vary according to the laboratory and the type of detector used. However, a trend of improving performance with time can be observed which might be due to corresponding improvements in the manufacturing of the mMLC leaves, and the use of better techniques and detectors to measure these properties.

The Results show that average values of transmission and leakage radiation are 0.93 ± 0.07% and 1.08 ± 0.08%, respectively. The 80-20% beam penumbra were found to be 2.26 ± 0.11 mm along the leaf side and 2.31 ± 0.11 mm along the leaf end using square field sizes ranging from 9.1 to 1.8 cm. These measurements are in agreement with those reported in the literature using different radiation detectors. The results on this work show that some of the basic dosimetric properties of the m3-mMLC for stereotactic radiosurgery and radiotherapy applications can be measured with high precision using GafChromic EBT radiochromic film. These films have several advantages when compared to other detectors, namely, they have high spatial resolution and sensitivity, their responses independent of photon energy, and their readout can be performed with relatively cheap equipment. However, it is important to use a very strict protocol for the handling and readout of the films if reproducible and high precision results are to be obtained.

Chapter three

Methodology

This is an experimental study conducted to assess the radiotherapy treatment beam using computer programs.

3.1. Materials:

3.1.1. Cobalt-60 machine:

- This study was conducted at radiotherapy department, Radiation and Isotopes Center of Khartoum (RICK), Khartoum state, Sudan, from July 2014 up to December 2014. In order to assess the radiotherapy beam using portal film and by measuring the field size and the penumbra size and the uniformity of the beam. Linear accelerator machine (ELECTA) 10 Mv
- Co-60 (1) EQUINOX source size 2.5×1.5×1.5 cm
- Activity 1×1×1 cm

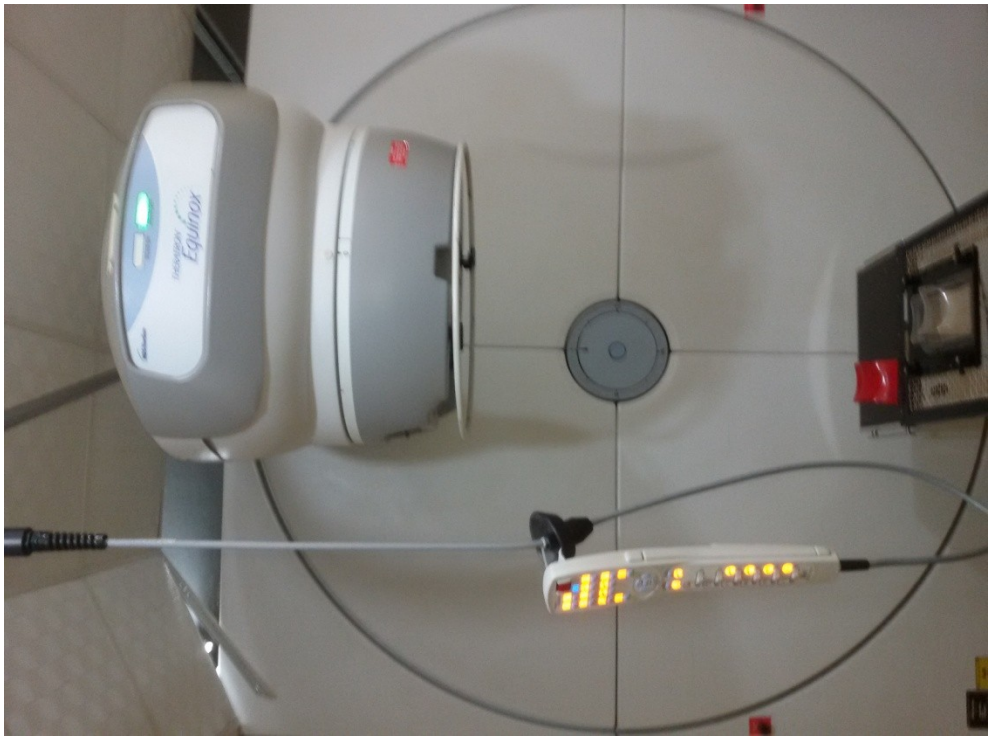

- Co-60 (2) MDS source size 1×1×1 cm

  0.75×0.75×0.75 cm

  Focus 1 cm

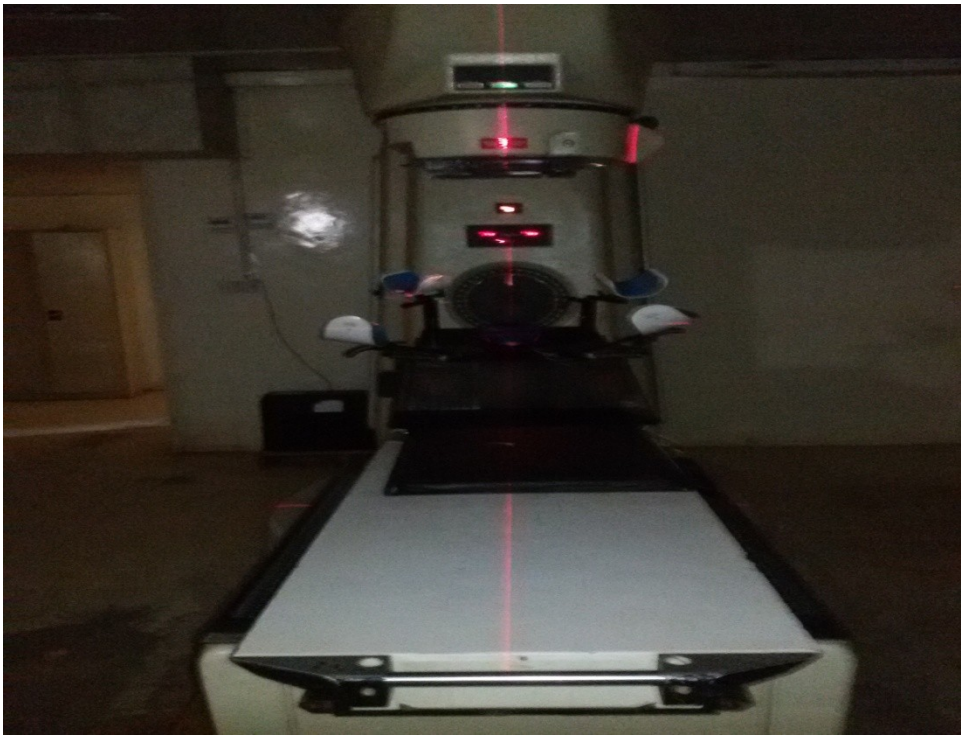

3.1.2. A linear particle accelerator:

- Linear accelerator machine (ELECTA) 10 Mv

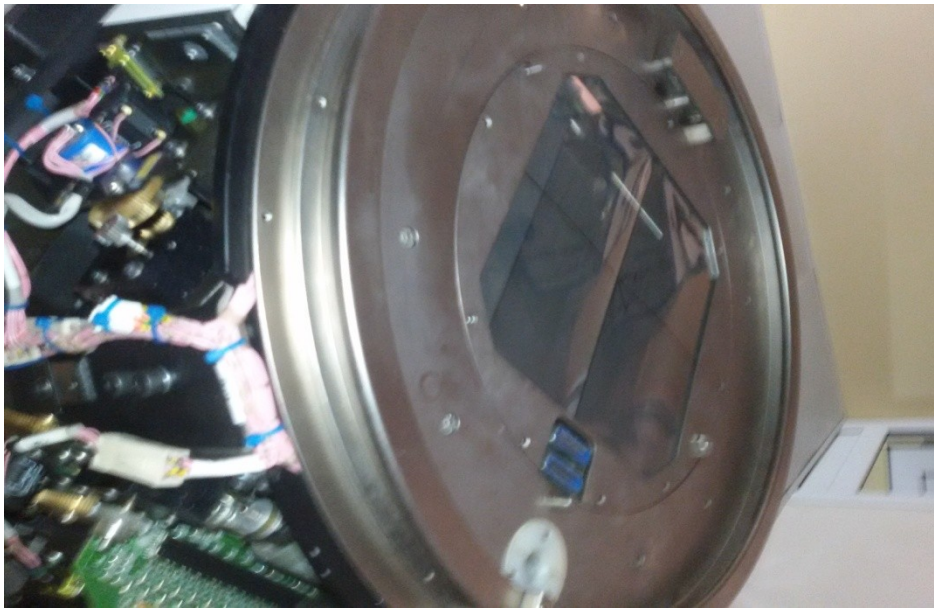

3.2 Design of the study:

Experimental descriptive study

3.3 Sample size and type:

- Linear accelerator machine (ELECTA) 10 Mv
- Linear accelerator machine (ELECTA) 10 Mv
- Co-60 (1) EQUINOX source size 2.5×1.5×1.5 cm

  Activity 1×1×1 cm
- Co-60 (2) MDS source size 1×1×1 cm

  0.75×0.75×0.75 cm

Focus 1 cm

3.4 Place of the study:

The study was conducted at radiotherapy department, Radiation and Isotopes Center of Khartoum (RICK), Khartoum state, Sudan.

3.5 Duration of the study:

The study was carried out from July 2014 up to December 2014.

3.6 Method of data collection (technique):

for radiotherapy machine (CO-60) and linear accelerator, each film scanned using digitizer scanner then treated by using image processing program (IDL), where the field size and penumbra and the uniformity of radio therapy beam will be determined, accelerator for vertical and horizontal reading on The portal films, with SSD = 100cm and the field size 10 ×10 cm^2 and isocentric set-up 0^0-90^0,270^0

3.7 Variable of the study

The variable of the study was the field size, the penumbra size, and percentage of the field size, reduced area from the field size, Dose percentage in the field and Dose percentage in the border of the field.

Chapter Four

Results

The results show radiographic images with Linear accelerator machine (ELECTA) 10 Mv , and two type of cobalt-60 machines Co-60 (1) EQUINOX source size 2.5×1.5×1.5 cm Active size 1×1×1 cm and the second type Co-60 (2) MDS source size 1×1×1 cm 0.75×0.75×0.75 cm, with Focus 1 cm .

And illustrating the 10×10 cm field size, and two regions of penumbra, and the percentage of the dose in the field, and show the reduced area from the field size of co-60 and show that no area reduced from the field size of linear accelerator

Table 4.1 measured field size and the percentage of the radiation received

%	Field reference (10*10)cm	Machine
94.1766 %	9.41766×9.41766 cm	Co- 60
91.1417 %	9.11417×9.11417 cm	Co-60
100 %	10.0×10.0 cm	Linear
100 %	10.0×10.0 cm	Linear

Table 4.2 area reduced from reference field size

Machine	Reduced area from the field size
Co- 60	0.58234 cm
Co-60	0.88583 cm
Linear	0.0000
Linear	0.0000

Table 4.3 Percentage of the field received radiation by 100%

Machine	Dose percentage in the field	Dose percentage in the border of the field
Co- 60	98.039 %	83.137 %
Co-60	94.118 %	89.02 %
Linear	78.431%	---------
Linear	78.431%	---------

Table 4.4 penumbra size

Machine	Penumbra size
Co- 60	1.224
Co-60	1.0363
Linear	0.4517
Linear	0.4637

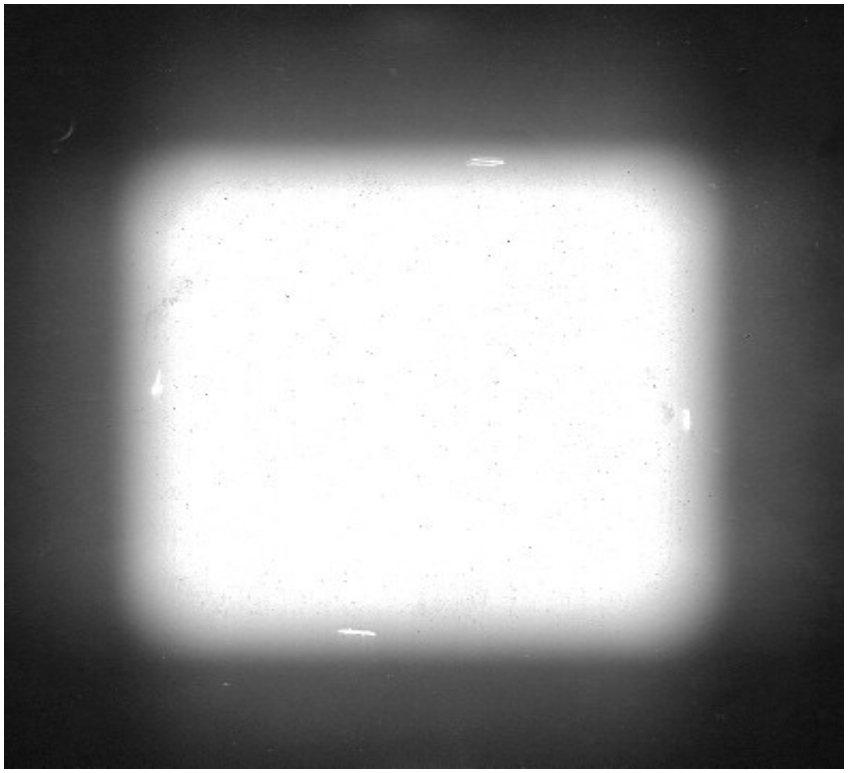

Fig 4.1 radiographic image with Co-60,
Measured field size was 9.41766×9.41766 cm, 94.1766 % .

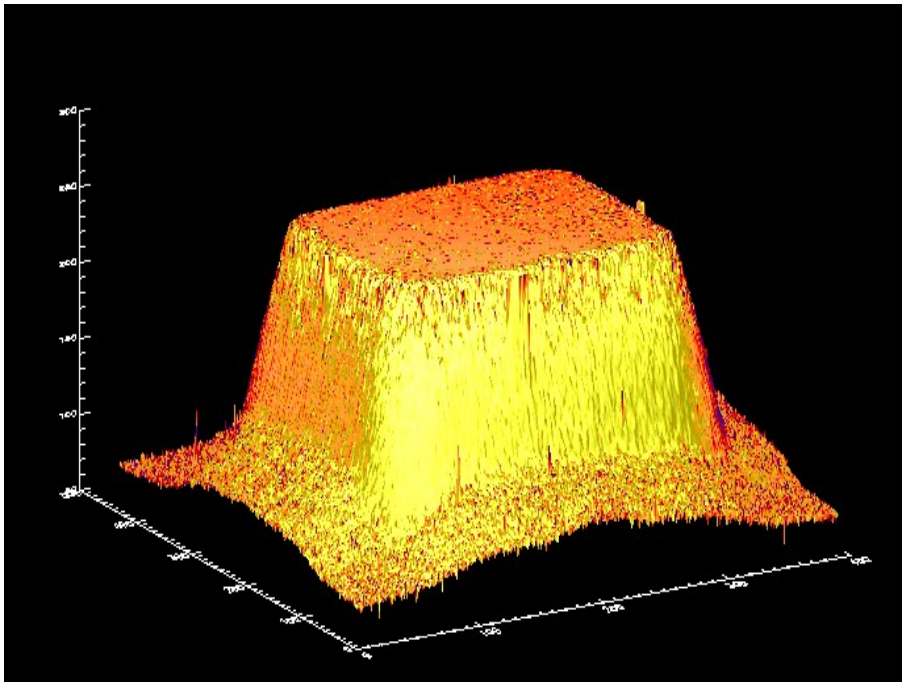

Fig 4.1.a histogram showing the reduced area from the reference field size in co-60 machine and it was
0.58234 cm

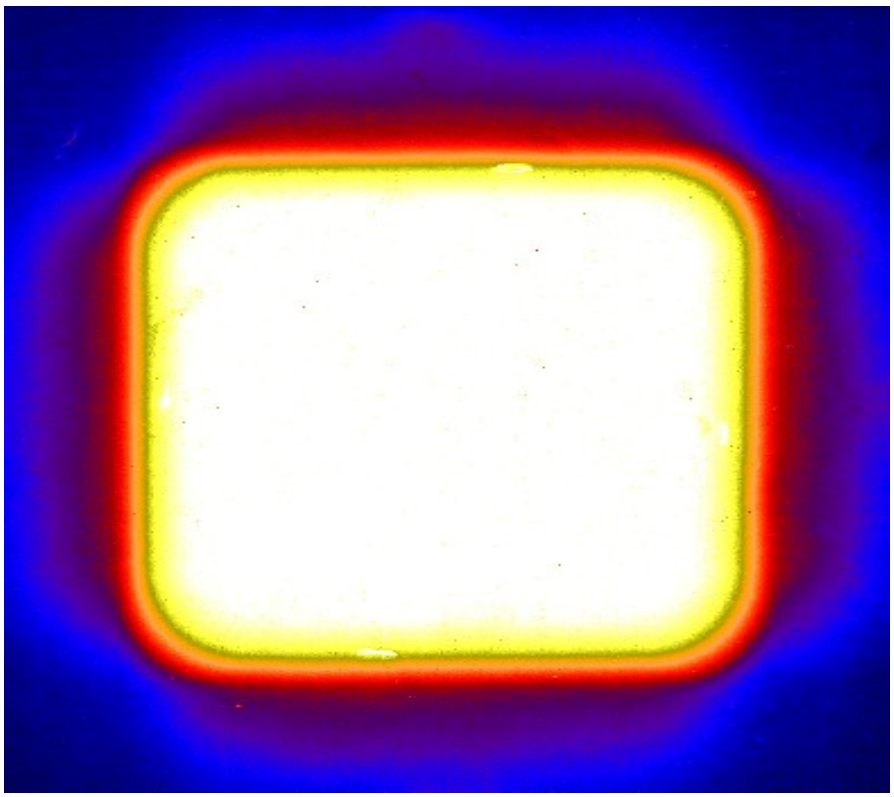

Fig 4.1.b field size 9.41766×9.41766 cm, 94.1766 % with white color, border of the field with yellow and penumbra region 1.224 cm with orange and red color

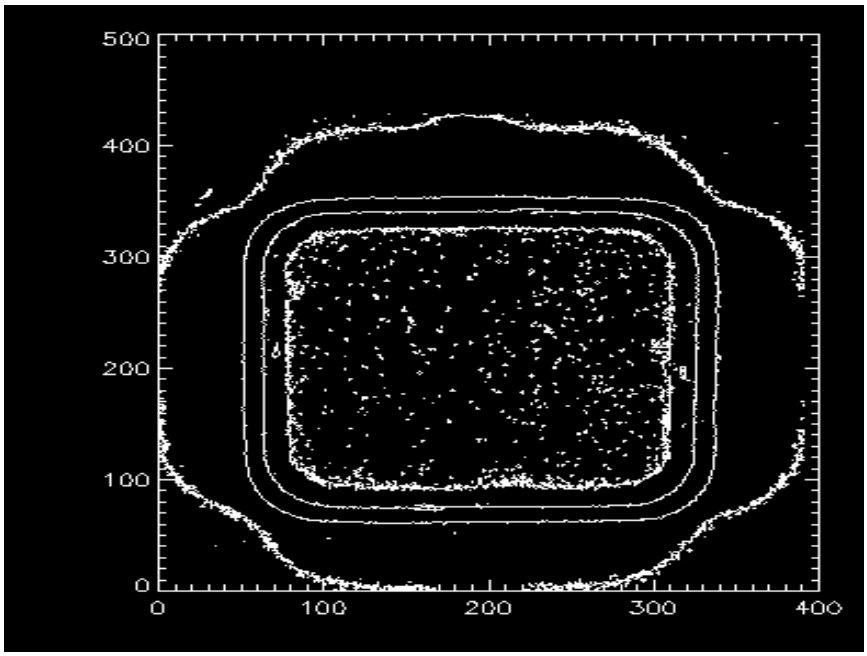

Fig 4.1.c contour for the image

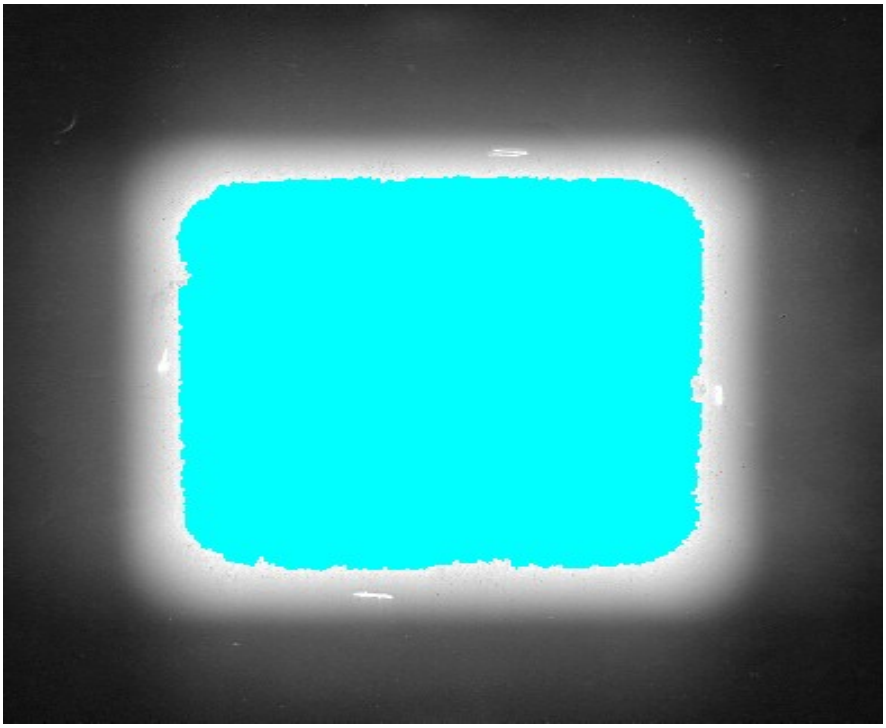

Fig 4.1.d percentage of the dose in the field was 98.039 % and in the border 83.137 %
For Co-60 machine.

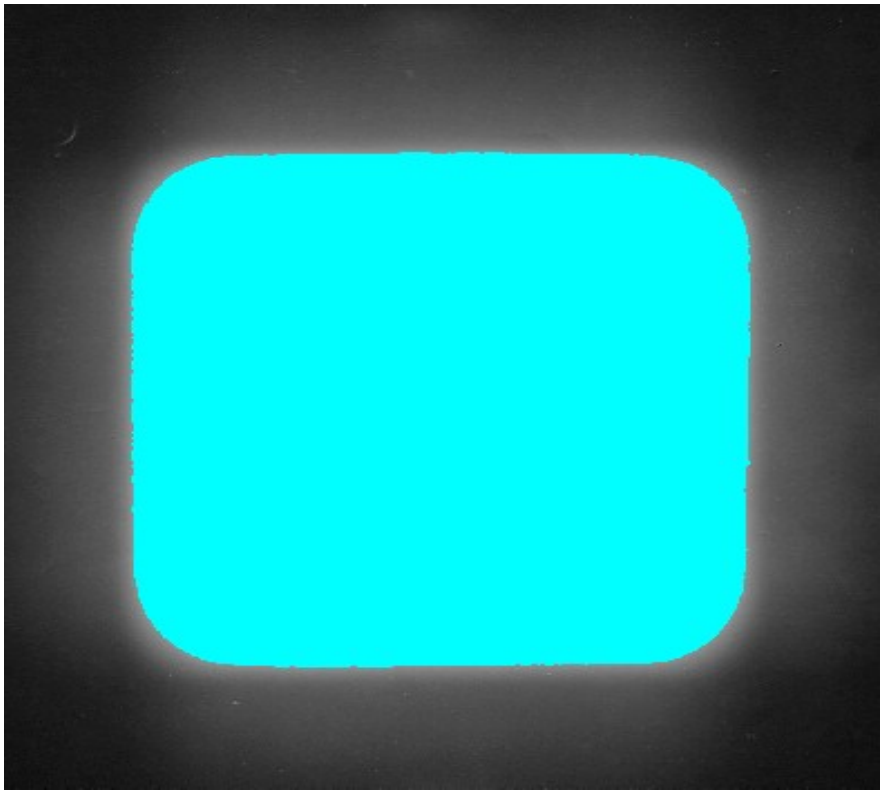

Fig 4-1-e, the field size 10 × 10 cm.

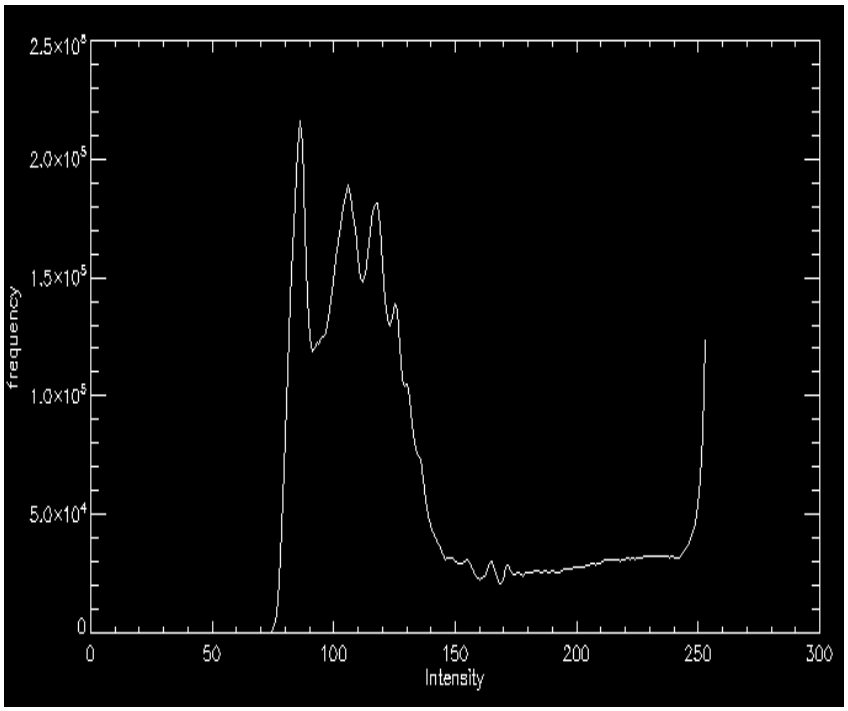

Fig 4-1-f, histogram showing scatter and penumbra region

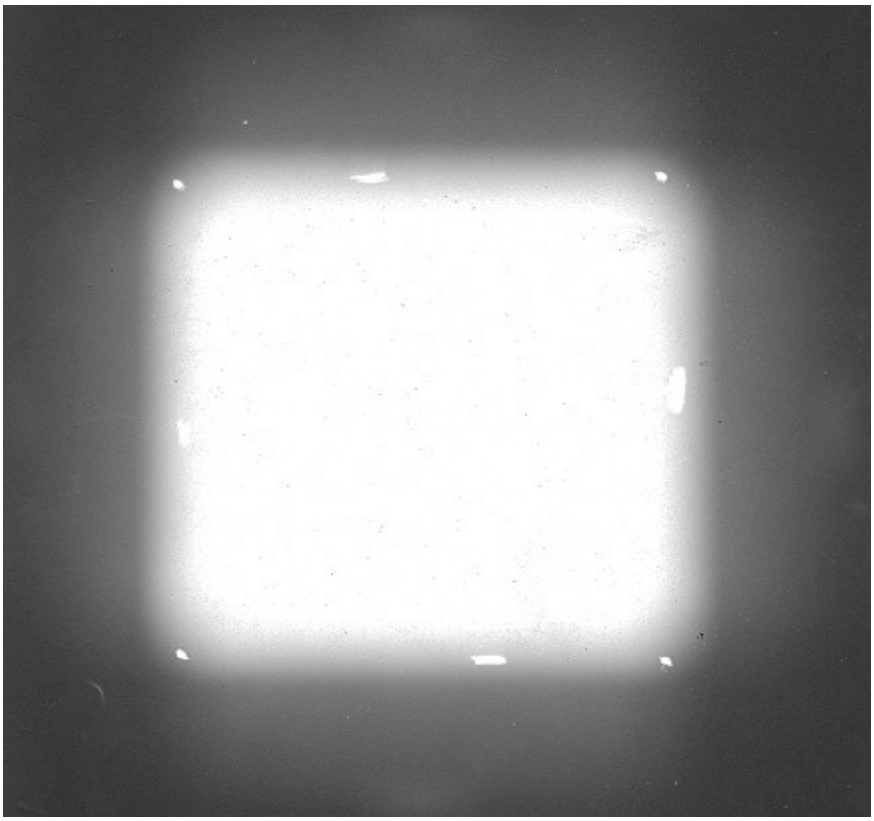

Fig 4.2 radiographic image with Co-60,
Measured field size was 9.11417×9.11417 cm and 91.1

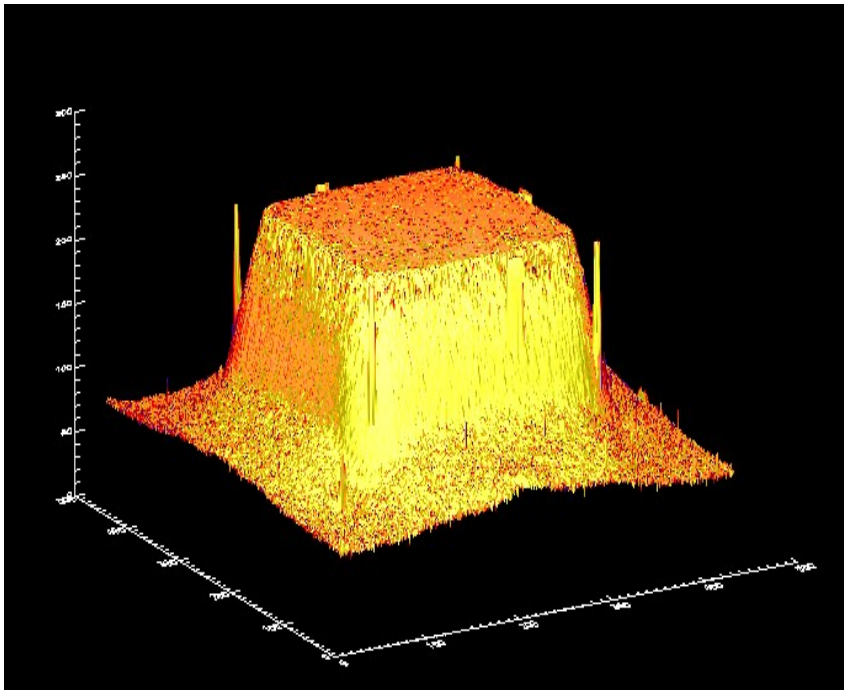

Fig 4.2.a histogram showing the reduced area from the reference field size in co-60 machine and it was 0.88583 cm

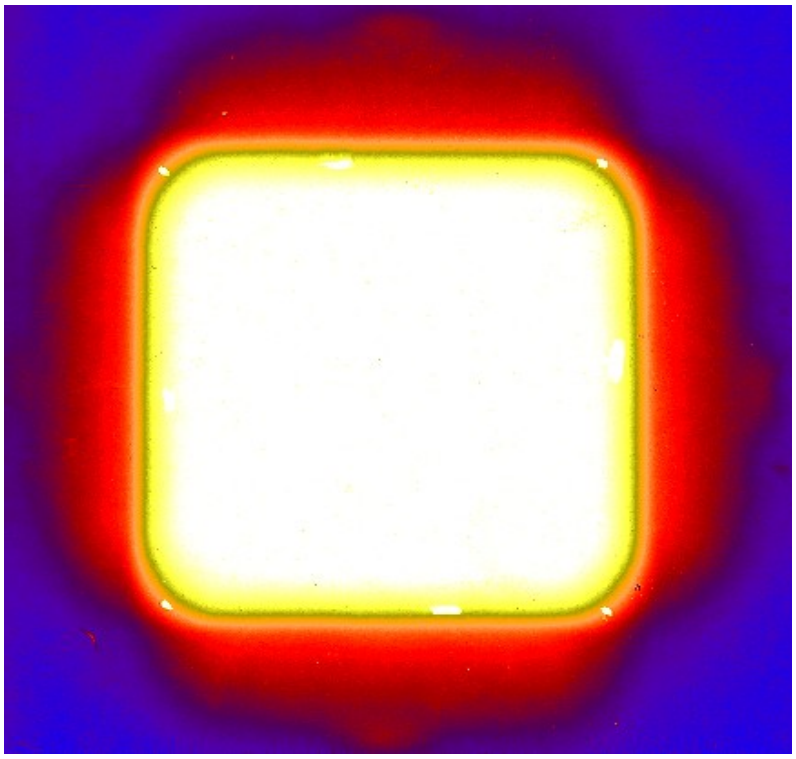

Fig 4.2.b useful field size 9.11417×9.11417 cm with white color, border of the field with yellow and penumbra region 1.0363 cm with orange and red color.

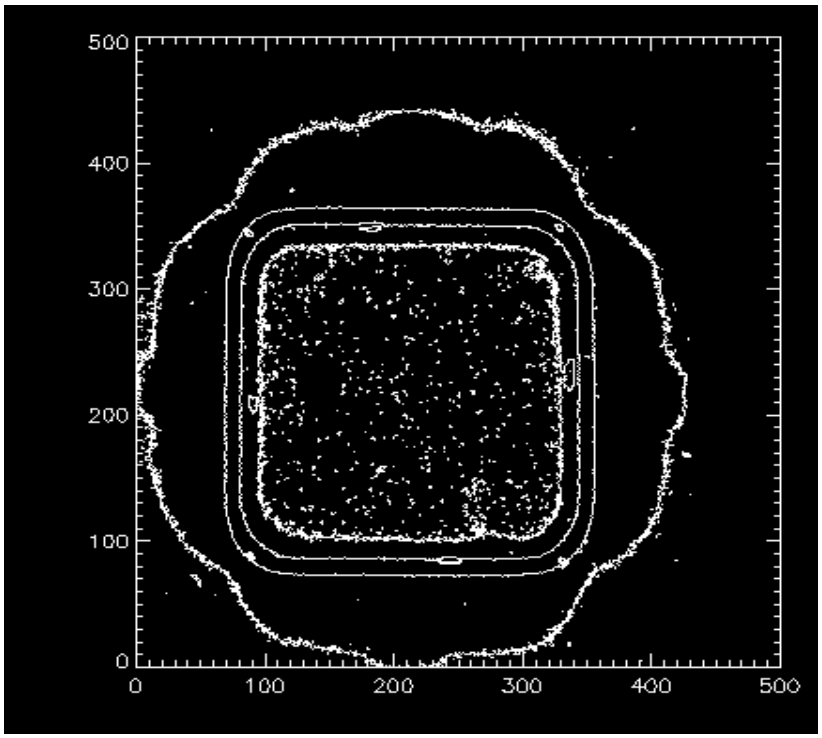

Fig 4.2.c contour for the image

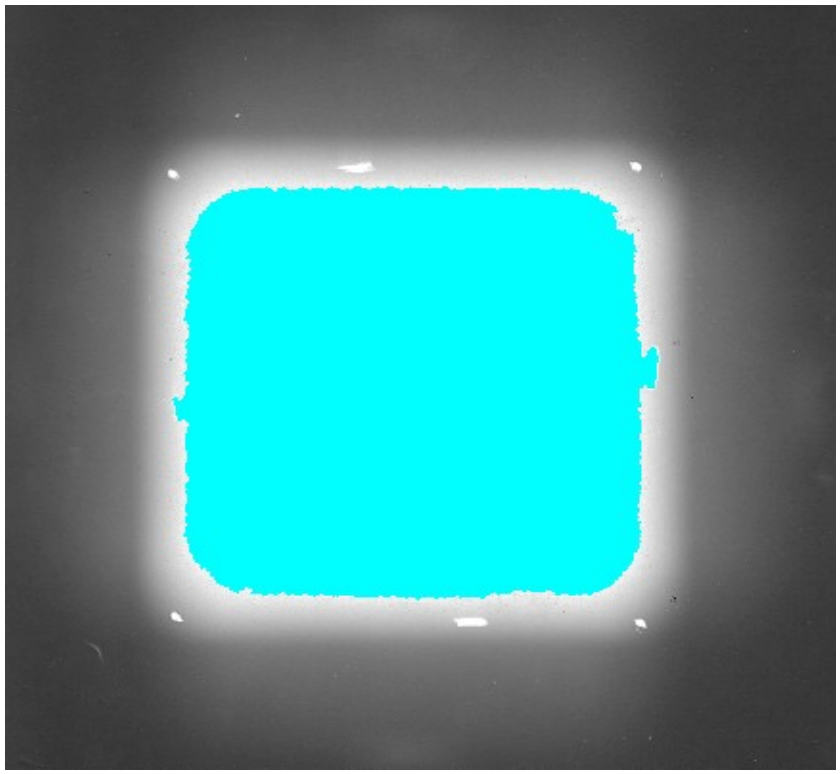

Fig 4.2.c percentage of the dose in the field was 94.118 % and in the border 89.02 %

For Co-60 machine.

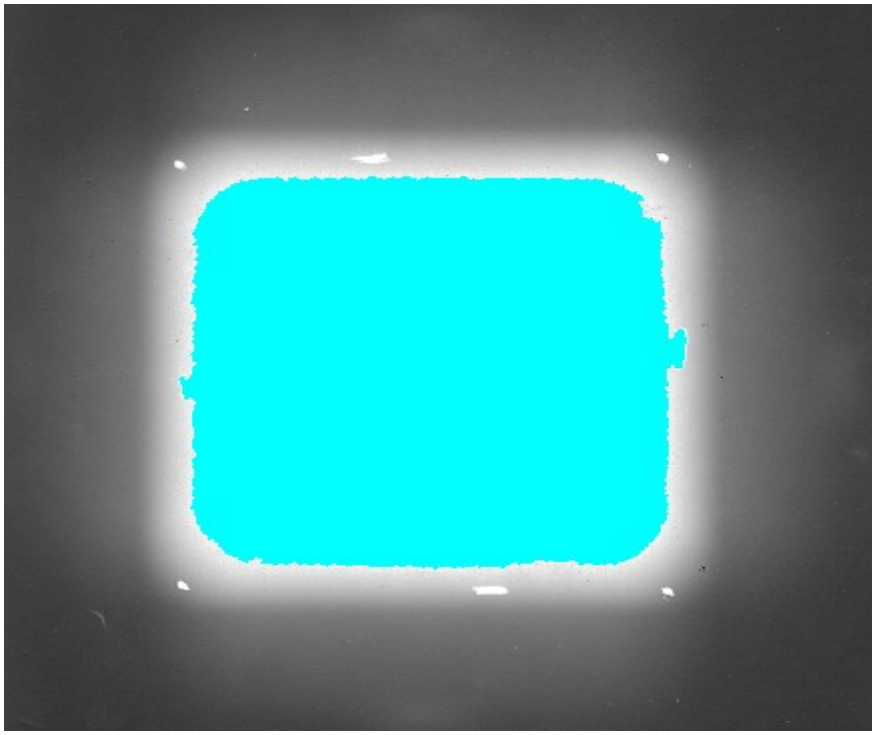

Fig 4.2.e percentage of the dose in the field was 94.118 % and in the border 89.02%
For Co-60 machine.

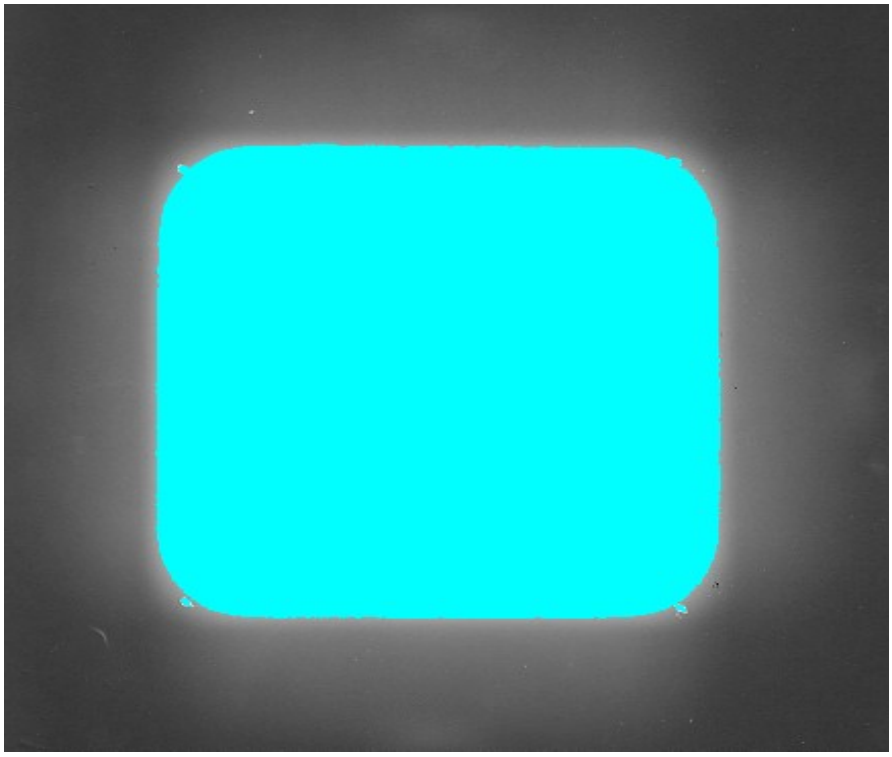

Fig 4.2.f the field size 9.11417×9.11417 cm

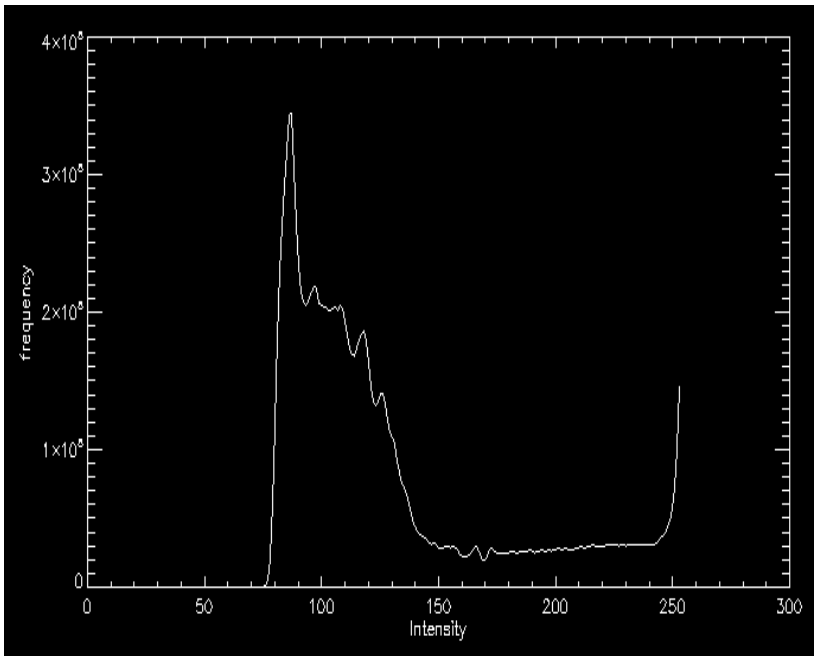

Fig 4.2.g histogram showing scatter and penumbra region

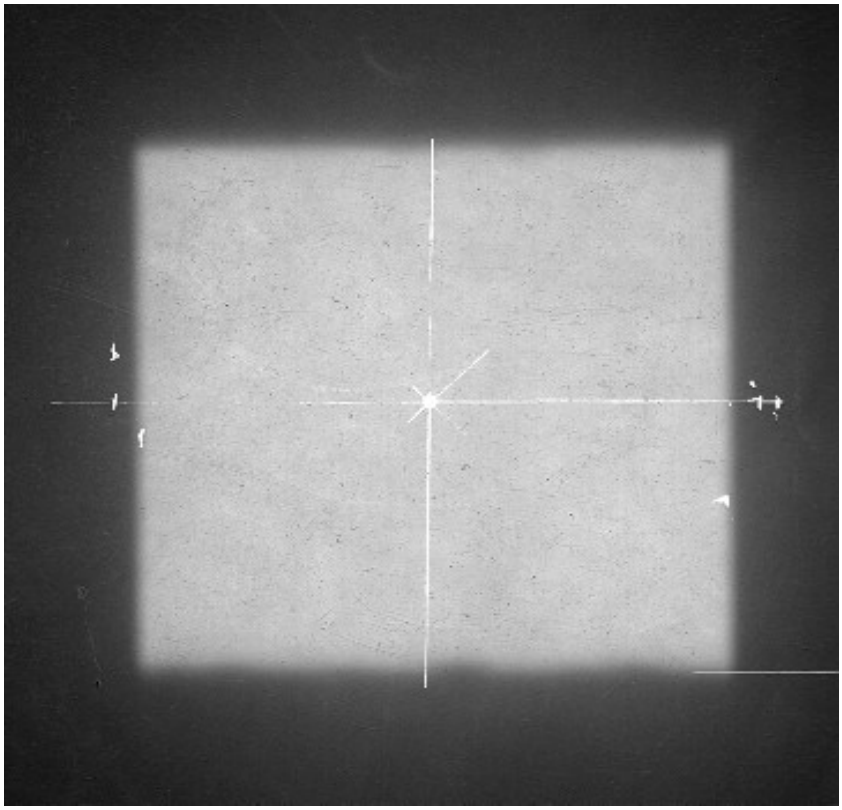

Fig 4.3 radiographic image with linear accelerator, measured field size was 10×10

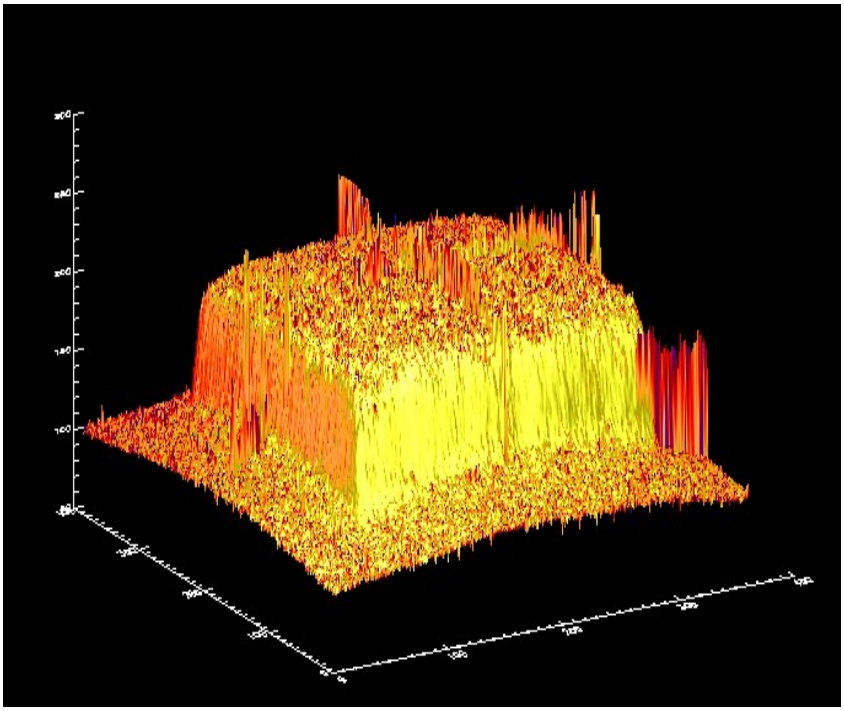

Fig 4.3.a histogram showing the reduced area from the reference field size for linear accelerator
Machine and it was 0.000 cm

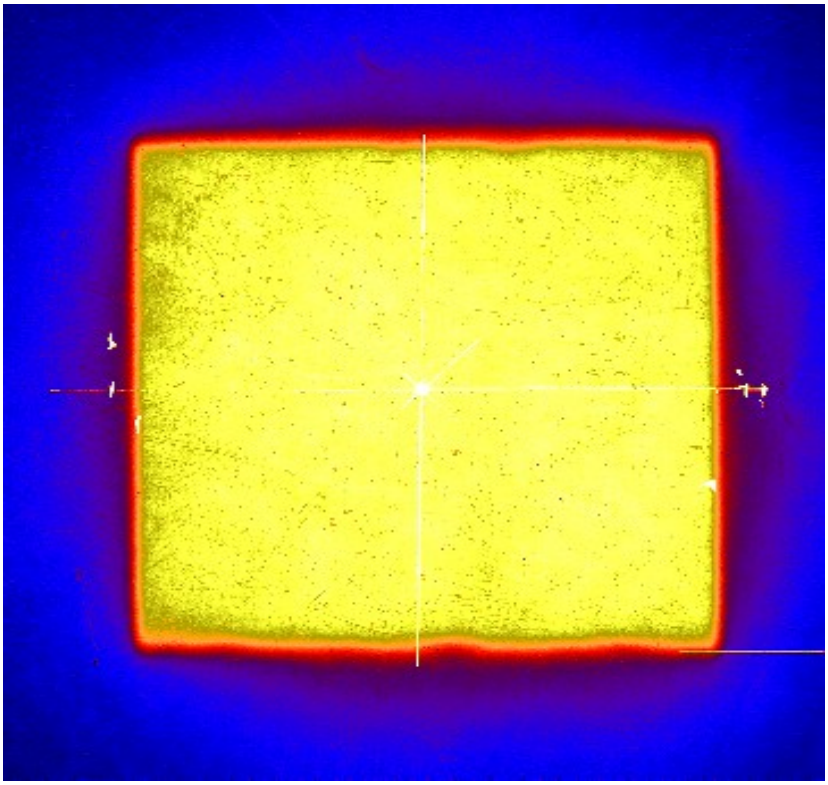

Fig 4.3.b useful field size10×10 cm with white color, border of the field with yellow and penumbra region0.4517 with orange and red color

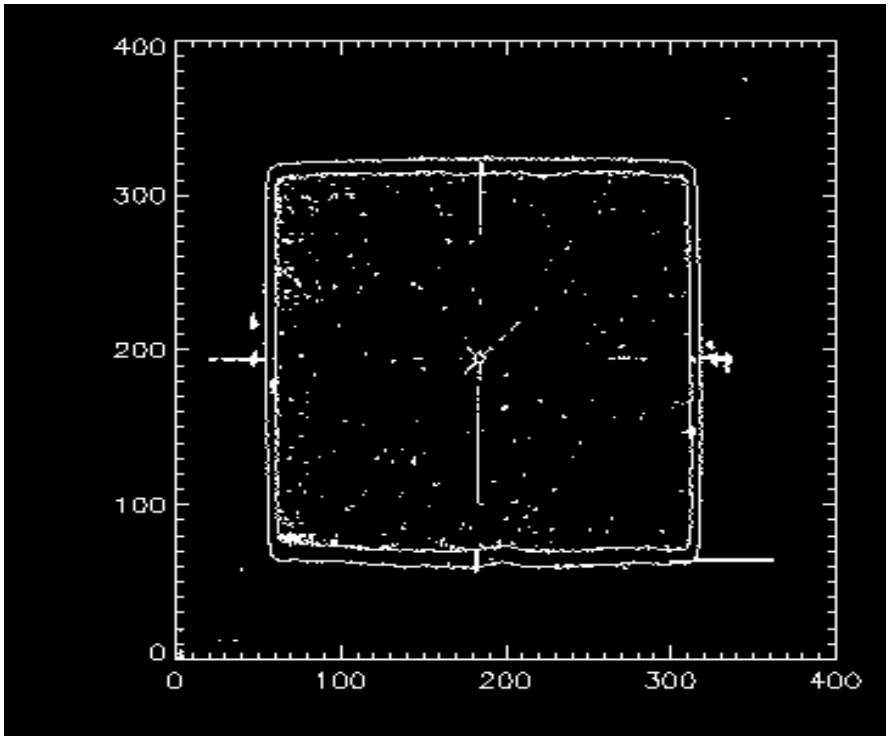

Fig 4.3.c contour for the image

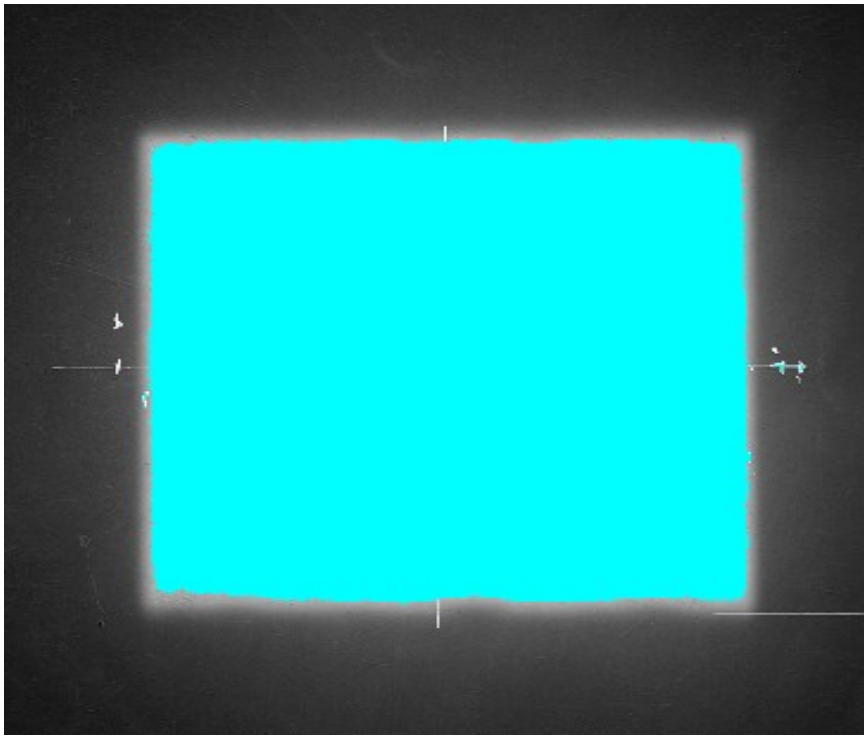

Fig 4.3.d percentage of the dose in the field was 78.431% and in the border 0.000 %
For linear accelerator machine.

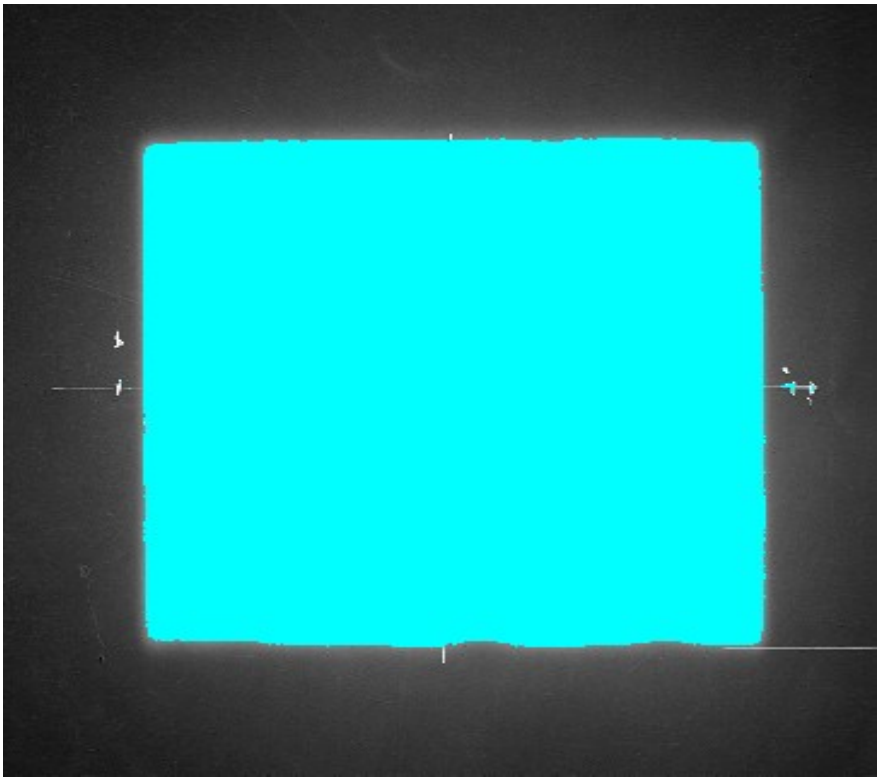

Fig 4.3.e the size 10×10 cm

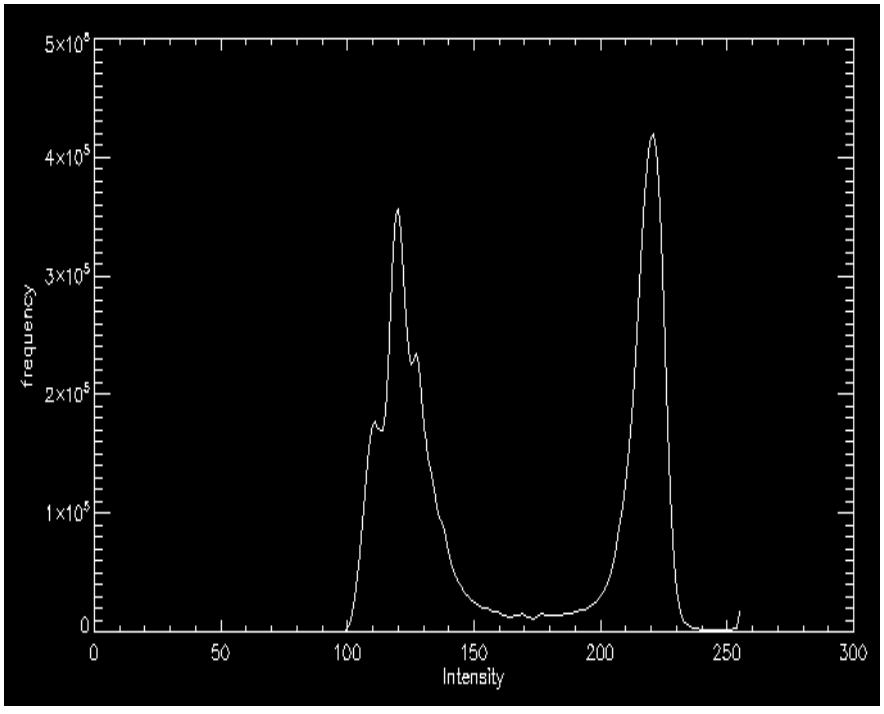

Fig 4.3.f histogram showing scatter and penumbra region

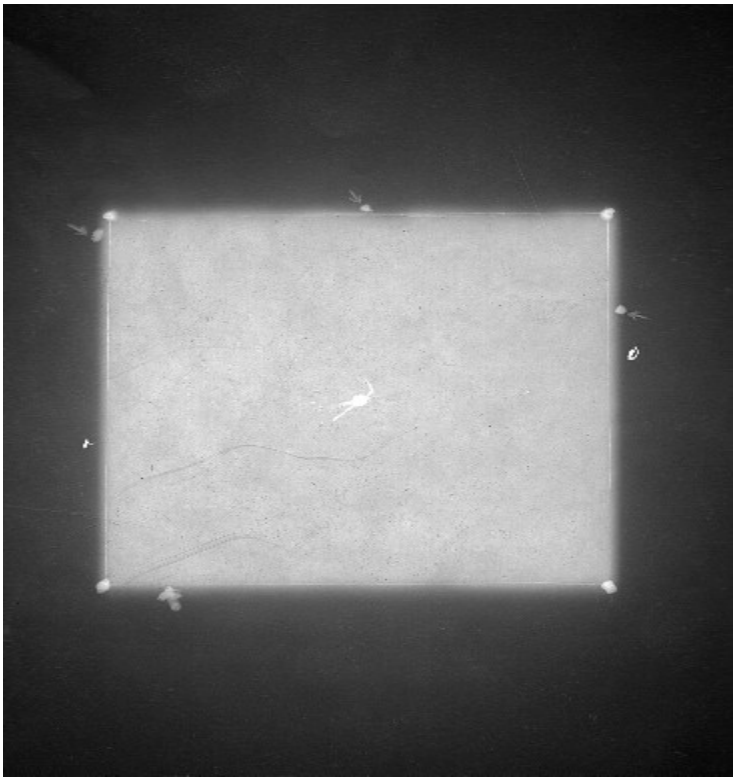

Fig 4.4 radiographic image with linear accelerator measured field size was 10×10 cm

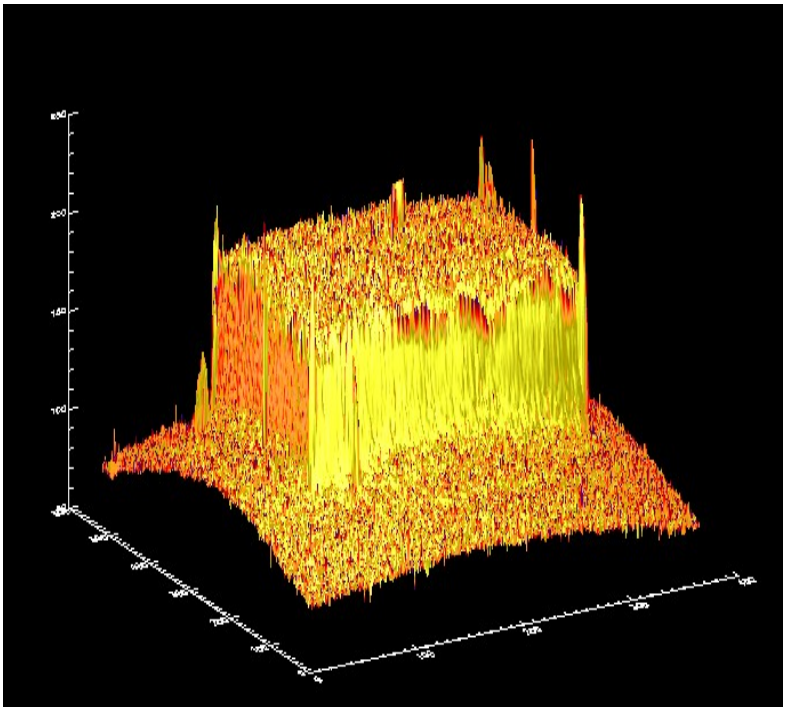

Fig 4.4.a histogram showing the reduced area from the reference field size for linear accelerator

Machine and it was 0.000 cm

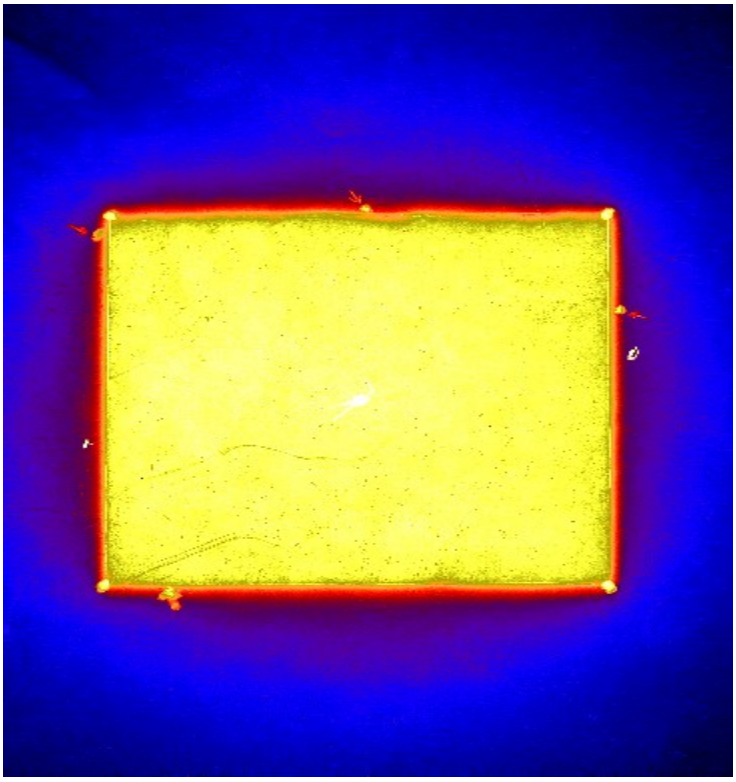

Fig 4.4.b useful field size 10×10 cm with white color, border of the field 0.000cm with yellow and penumbra region with orange and red color

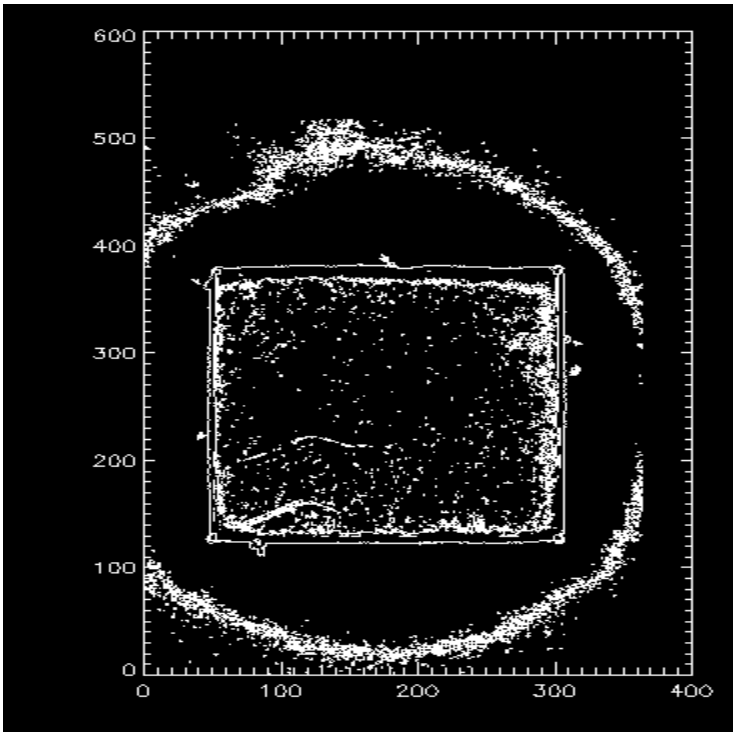

Fig 4.4.c contour for the image

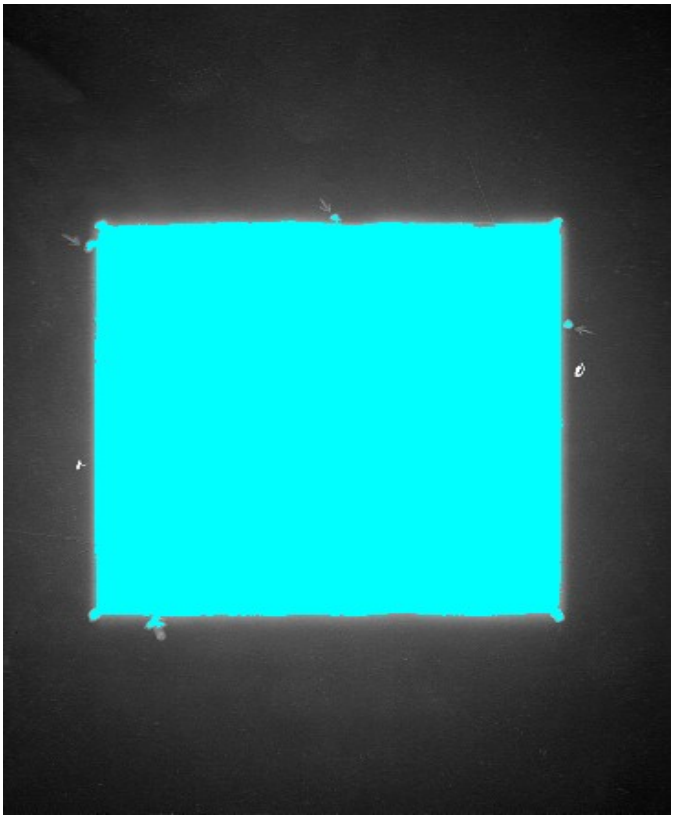

Fig 4.4.d percentage of the dose in the field was 78.431% and in the border 0.000 %

For linear accelerator machine.

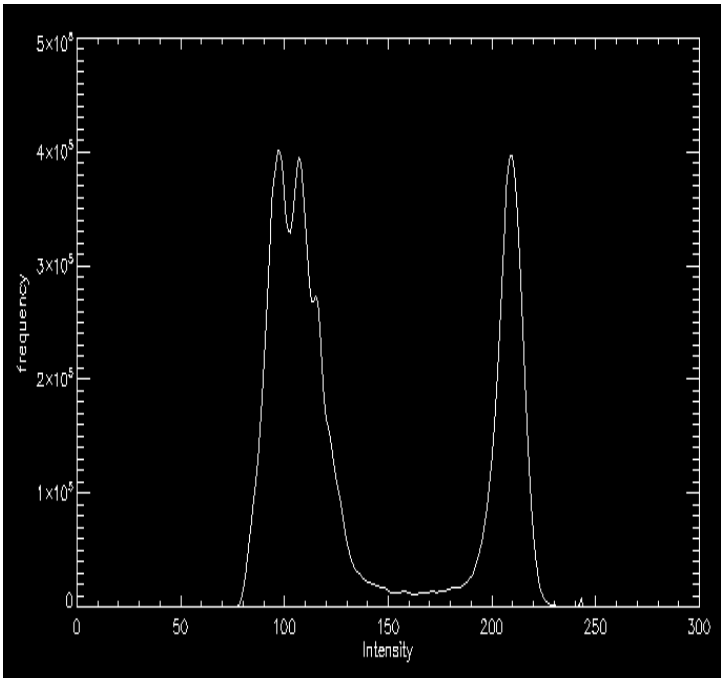

Fig 4-4-e, histogram showing scatter and penumbra region

Chapter five

Discussion, conclusion and recommendation

This study was performed by using two type Linear accelerator machine (ELECTA) 10 Mv Linear accelerator machine (ELECTA) 10 Mv Co-60 (1) EQUINOX source size 2.5×1.5×1.5 cm Activity 1×1×1 cm Co-60 (2) MDS source size 1×1×1 cm 0.75×0.75×0.75 cm and Focus 1 cm.

The images processed using (IDL) program to measure field size, the penumbra size, and percentage of the field size, reduced area from the field size, Dose percentage in the field and Dose percentage in the border of the field.

5.1 Discussion:

This study was performed to assess the radiotherapy beam by measuring the field size, the penumbra size and the percentage of the field dose. The results of these study showed that the field size of the two types of co60 machine was measured as (Yousif M et. Al 2014), and it was found to be (9.4×9.4) cm and (9.1×9.1) cm, the reduction in field size was 0.58234 cm in first type and 0.88583 cm in the second one and its means that the verification light and field size doesn't matched and that due to adjustment error in the machine (mechanical error), for linear accelerator machines the field size was measured to be 10×10 cm exactly as the reference field size, and there is no area reduced in linacs.

The penumbra size for the two type of co 60 machine was measured also as (Olivia Amanda García-Garduñ et al. 2007), and (Se An Oh et al 2012)study, and it was 1.224 cm and 1.0363 cm, and the penumbra size of the linear accelerator machines was found to be 0.4637cm and 0.4517cm as Tsang Cheung et al, 2006, and this also matched with (Olivia Amanda García-Garduño et al 2007) study.

The area of the field that received radiation by 100% agreed with (Kron T et al 1993)study was measured and it was 94.1 % and 91.1 % in co60 and 100 % for linear accelerator machine and that means linacs machines deliver the 100% of the dose to the useful field size.

The dose percentage in the field for co-60 was 98.0 % and 94.1 % and thus the dose in the border of field 83.1 % and 89.0 % , it's different in linacs because the

dose percentage in the field was 78.431% and 78.431% and there is no measurable dose outside the field size of linacs.

5.2 Conclusion:

Digital image processing has the potential to enhance and improve several functions of a modern radiation oncology department. These functions may include improving perception of information for films, electronic transfer of images to remote facilities and back, and reducing storage space requirements for archiving once treatment is finished.

From the result it was found that the cobalt-60 machine has field size different from the reference one and has large penumbra size more than linear accelerator and this is due to the source size of co-60 the , but the Penumbra trimmers, a

beam accessory, can be placed closer to the patient surface to provide additional collimation and reduce the effect of the finite source size.

5.3 Recommendations:

• For accurate treatment planning process, field size verification should be done frequently.

• Periodic preventing maintenance of the machine should be done in order to detect changes in adjusting field size

• For future study assessment of radiotherapy beam by using non screen films produce an image with undesirable levels of blur and contrast.

• measurement of beam parameter can be done using different field size.

References

1- Yousif M. Y. Abdallah, Menas A. Boshara, (2014), Assessment of field size on radiotherapy machines using texture analysis. Department of Radiotherapy and

Nuclear Medicine, College of Medical Radiological Science, Sudan University of Science and Technology, Khartoum, Sudan , DOI: 10.4103/1858-5000.144642

2- Lin Y D and Stock K D, (2000), Thermopile detectors: spatial non-uniformity measurements and correction methods 2000 Metrologia 37 481. doi:10.1088/0026-1394/37/5/30

3- Leszczynski K, Shalev S, Gluhchev G, (2003), Verification of radiotherapy treatments: computerized analysis of the size and shape of radiation fields. PMID: 8350820

4- Se A O,Min K K, Ji W Y, Sung K K and Young K O, (2012) Study of the penumbra for high-energy photon beams with Gafchromic™ EBT2 films ,Journal of the Korean Physical Society

5- Tsang C, Martin J. Butsona, Peter K. N. Yu,(2006), Measurement of high energy x-ray beam penumbra with Gafchromic™ EBT radiochromic film http://www.cityu.edu.hk/ap/nru/pub_j150.pdf

6- Murray A, Barnfield M, Thorley P , (2005) , Optimal uniformity index selection and acquisition counts for daily gamma camera quality control.

7- Keller B, Beachey D, Pignol J , (2007), Experimental measurement of radiological penumbra associated with intermediate energy x-rays (1 MV) and small radiosurgery field sizes. Med Phys. 2007 Oct; 34(10):3996-4002.

8- Kron T, Elliott A, Metcalfe P , (1993) ,The penumbra of a 6-MV x-ray beam as measured by thermoluminescent dosimetry and evaluated using an inverse square root function.PMID: 8289725 [PubMed - indexed for MEDLINE]

9- Suresh R, Hardev S,(2013), Impact of heterogeneities on lateral penumbra in uniform scanning proton therapy, International Journal of Cancer Therapy and Oncology (IJCTO) (ISSN 2330-4049) DOI: http://dx.doi.org/10.14319/ijcto.0102.6

10- Hatimbhai, Singh M, Iyer P, (1976), Effect of field size on the radiation penumbra and integral dose for telegamma therapy units. PMID: 1258085 [PubMed - indexed for MEDLINE]

11- Olivia A, García-G, Miguel Á, José M, Sergio M, Arnulfo M and Mercedes R, (2007), Radiation transmission, leakage and beam penumbra measurements of a micro-multileaf collimator using GafChromic EBT film mercedes@fisica.unam.mx

12- Marks, J.E., Haus, A.G., Sutton, H.G., Griem, and M.L, (2006), the value of frequent verification films in reducing localization error in the irradiation of complex fields, Cancer 37: 2755-2761, 1976.

13- World Academy of Science, Engineering and Technology

Vol: 5 2011-08-28 (Vahid Fayaz , Hassan Zandi)

14- Quality Control of Scintillation Cameras (Planar and SPECT) Michael K. O'Connor, Mayo Clinic, Rochester, MN

Appendix

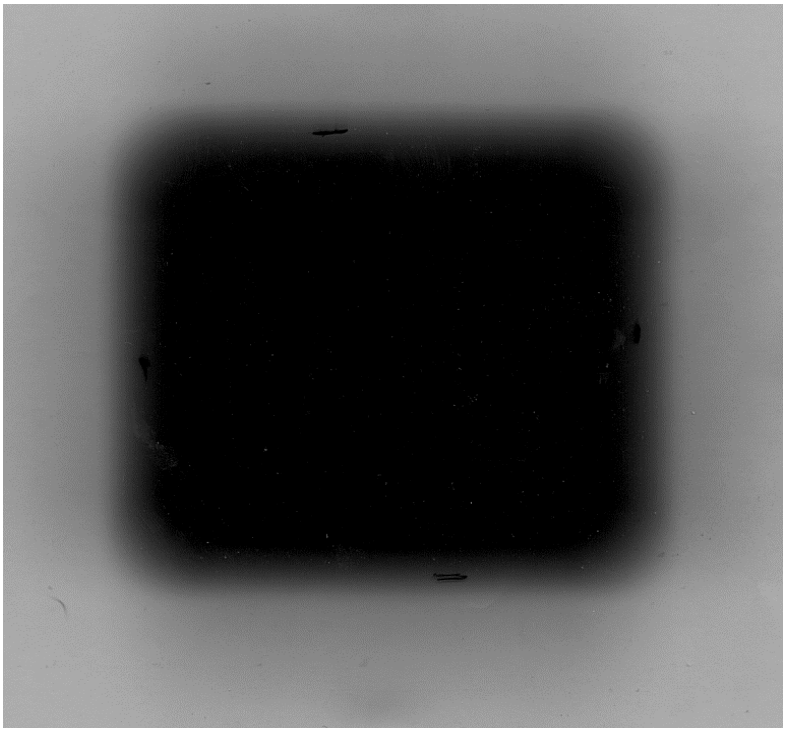

Radiographic image with co-60 , field size 10×10 cm and SSD=100 cm.

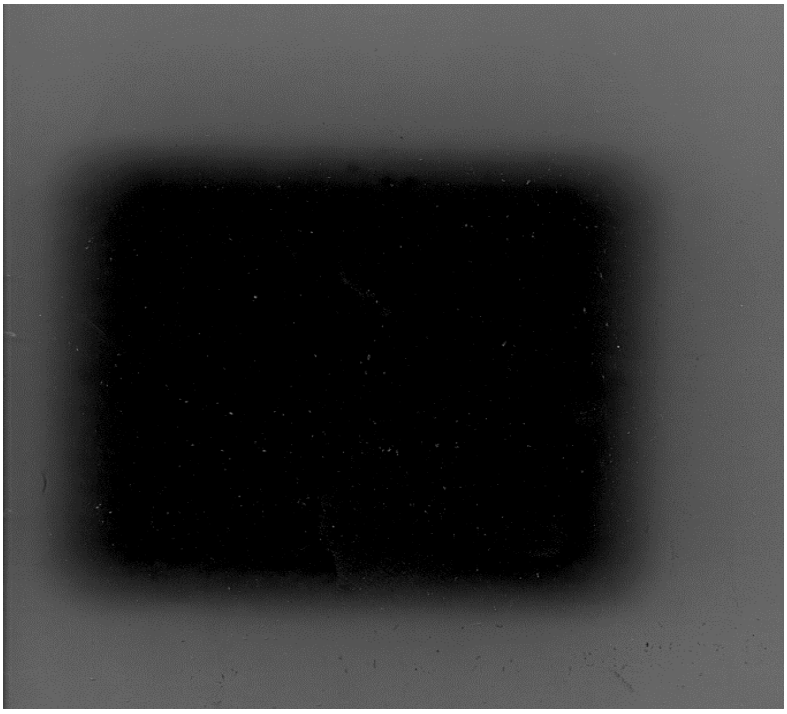

Radiographic image with co-60 , field size 10×10 cm and SSD=100 cm.

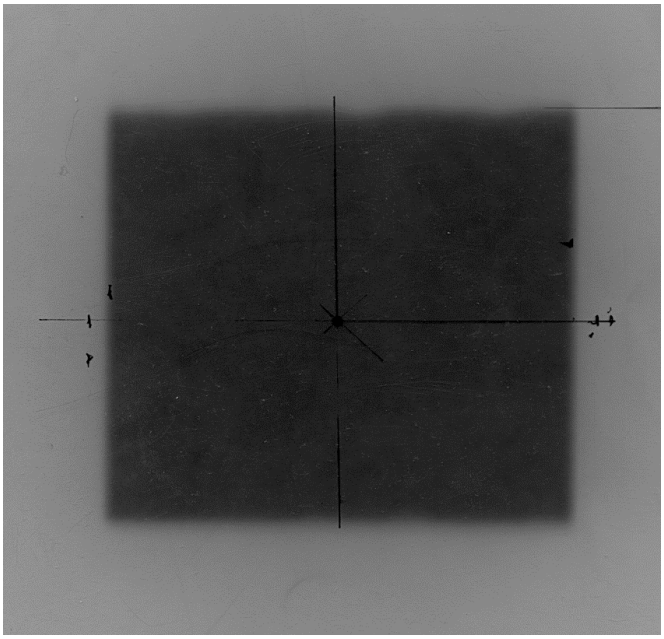

Radiographic image with linear accelerator machine ,

field size 10×10 cm and SSD=100 cm.

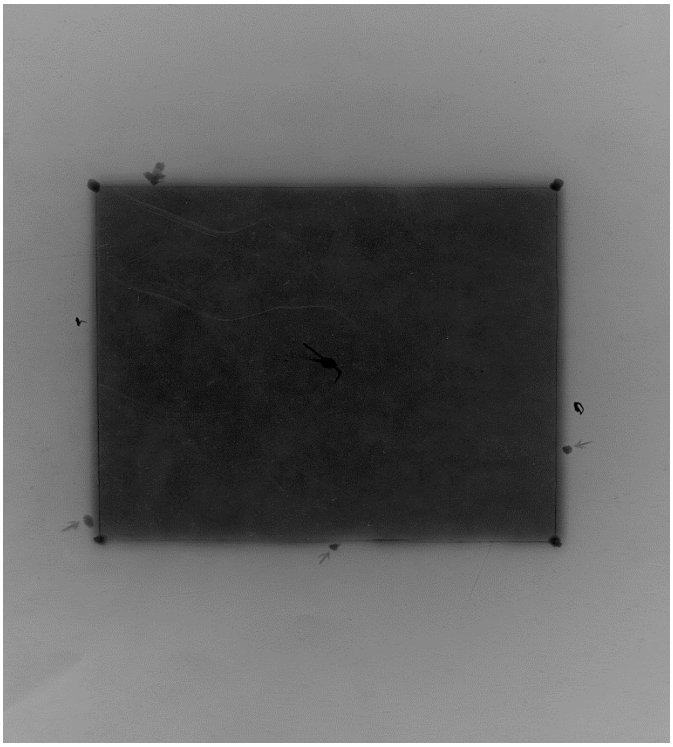

Radiographic image with linear accelerator machine ,

field size 10×10 cm and SSD=100 cm.